Table 2. Characteristics of patients receiving allogeneic hematopoietic stem cell transplantation (*n* = 46)

Characteristics	
Median age of patients (range), years	53 (18–62)
Sex of recipient (%)	
Male	29 (63)
Female	17 (37)
Sex, donor versus recipient (%)	
Match	25 (54)
Male to female	11 (24)
Female to male	10 (22)
Disease type (%)	
AML	24 (52)
1st CR	5
2nd CR	10
1st relapse	5
No treatment†	4
MDS	16 (35)
RA	4
RAEB	9
CMML	1
RAEB-t	2
CML	6 (13)
CP	5
AP	1
Disease risk‡ (%)	
Standard	14 (30)
High	32 (70)
Performance status§ (%)	
0	40 (86)
1	6 (13)
2	0 (0)
Donor (%)	
Related	19 (41)
Unrelated	27 (59)
HLA (%)	
HLA identical sibling	19 (41)
HLA 6/6 matched, unrelated	23 (50)
HLA mismatched, unrelated	4 (9)

†Two patients with overt leukemia from myelodysplastic syndrome (MDS) and another two patients with hypoplastic AML did not receive induction chemotherapy before transplantation. ‡Standard risk was defined as AML in 1st complete remission (CR), MDS in refractory anemia (RA) or RA with ringed sideroblasts, and CML in chronic phase (CP). §According to Eastern Cooperative Oncology Group criteria. AP, accelerated phase; CMML, chronic myelomonocytic leukemia; HLA, human leukocyte antigen; RAEB, refractory anemia with excess of blasts; RAEB-t, RAEB in transformation.

Table 3. Summary of transplantation in patients with AML (*n* = 24), myelodysplastic syndrome (*n* = 16), or CML (*n* = 6)

Stem cell source	
G-PBMC	7
Bone marrow	39
GVHD prophylaxis†	
sMTX+CyA	22
sMTX+FK	21
aGVHD, grade (%)	
None	26 (56)
I	4 (9)
II	11 (24)
III	4 (9)
IV	1 (2)
cGVHD, type (%)	
None	16 (43)
Lmt	9 (24)
Ext	12 (32)

†One patient received short-term methotrexate + tacrolimus prophylaxis and subsequently received short-term methotrexate + cyclosporine. aGVHD, acute graft versus host disease; chronic GVHD, chronic graft versus host disease; GVHD, graft versus host disease.
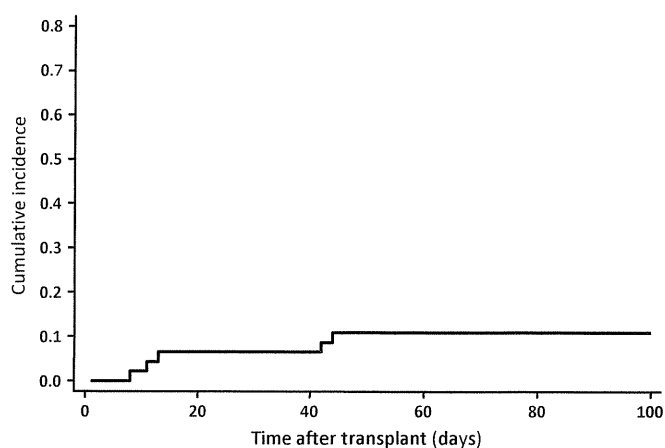

Fig. 1. Cumulative incidence of sinusoidal obstruction syndrome in patients receiving allogeneic hematopoietic stem cell transplantation treated with targeted oral busulfan and cyclophosphamide. The cumulative incidence of overall sinusoidal obstruction syndrome was 11% (95% confidence interval, 4–22%) at day 100 after transplantation.

diarrhea (30%) were frequent grade III or more adverse reactions. Severe neurological toxicity of grade III or more was observed in five patients (11%). One patient developed subarachnoid hemorrhage and died on day 1 after transplantation. Another patient developed tacrolimus encephalopathy on day 23 after transplantation. This patient died of acute bleeding from gastric ulcer on day 57. Another patient developed neurological toxicity during the course of septic shock and died on day 15. One patient who received dose reduction had delayed engraftment, but subsequently engrafted on day 31.

Among 46 patients undergoing planned transplantation, four patients experienced grade III or IV liver toxicity before day 28 (Table S1). Grade III or more long-term liver toxicity between days 29 and 100 was observed in nine patients (Table S2). Three patients were reported to have SOS before day 20, and two were reported to have late-onset SOS from days 21 to 100. Cumulative incidence of overall SOS was 11% (95% CI, 4–22%) at day 100 after transplantation (Fig. 1). Two patients had mild SOS on

day 8 and 11 after transplantation, and both improved. One of these patients died of an unrelated cause (acute renal failure and infection). The third patient was reported to have moderate SOS on day 13. This patient died of an unrelated cause (septic shock) on day 15 after transplantation. Two patients developed severe SOS on days 42 and 44. These patients died of hepatic failure on day 64 and 81, respectively.

Graft versus host disease. The cumulative incidence of grade II–IV and III/IV aGVHD at day 100 were 35% and 11%, respectively. The cumulative incidence of grades II–IV aGVHD in the recipients who underwent transplant from an HLA-identical related donor or unrelated donor was 26% and 41%, respectively, and those of grades III/IV aGVHD was 11% and 11%, respectively. The cumulative incidence of cGVHD at 1 year after transplantation was 52%. Of the 21 patients who developed cGVHD, 12 had extensive disease and nine had limited disease.

Survival outcome. Twenty-six patients were alive with a median follow-up of 43 months (range, 11.9–65 months) after

transplant. Overall survival was 65% (95% CI, 50–77%) at 1 year after transplantation, 66% (95% CI, 47–79%) for high risk and 64% (95% CI, 34–83%) for standard risk patients (Fig. 2a). Overall survival of AML was 71% (95% CI, 48–85%; $n = 24$) 1 year after transplantation, 50% (95% CI, 25–71%; $n = 16$) for MDS, and 83% (95% CI, 27–97%; $n = 6$) for CML patients. Two patients died before day 28 as described above. From days 28 to 100, seven patients died due to treatment-related mortality (four patients), infection (two patients), and relapse (one patient). Of the four patients who died of TRM, two died from hepatic toxicity, one from gastrointestinal bleeding, and one from thrombotic microangiopathy.

Disease-free survival was 57% (95% CI, 41–69%) 1 year after transplantation, 56% (95% CI, 38–71%) for high risk and 57% (95% CI, 28–78%) for standard risk patients (Fig. 2b). Disease-free survival of AML was 58% (95% CI, 36–75%) at 1 year, 44% (95% CI, 20–66%) for MDS, and 83% (95% CI, 27–97%) for CML patients.

Relapse and TRM. Thirteen patients (28%) experienced disease recurrence. Cumulative incidence of relapse was 24% at 1 year after transplantation. Cumulative incidence of relapse was 22% among patients with high risk disease, and 14% among patients with standard risk disease (Fig. 3a). Cumulative incidence of TRM was 18% at 1 year after transplantation (Fig. 3b).

Pharmacokinetic studies and dose modification. Among the 47 patients who completed the 16 BU doses, Css of the first dose was 1090 ± 318 ng/mL (range, 593–1673). The mean AUC_{inf}

estimated after the first dose of BU was 6760 μg·h/L (range, 3656–13058 μg·h/L). The mean values of oral clearance, distribution volume, and elimination half-life were 0.159 L/h/kg (0.079–0.263 L/h/kg), 0.55 L/kg (0.178–0.989 L/kg), and 2.54 h (0.98–5.49 h), respectively. Six patients received dose escalation of BU, and 32 received dose reduction (Fig. 4a). Median decreasing dose of BU was 4.5 mg/kg (28% of 16 mg/kg). Mean actual dose of BU was 12.7 ± 3.7 mg/kg (range, 7.6–21.3 mg/kg).

One patient was excluded from the analysis due to systemic convulsions on day −6, as described above. The Css of the first dose was 683.1 ng/mL in this patient. Although dose escalation was carried out to receive 18.7 mg/kg, the conditioning regimen was not completed.

Busulfan targeting and transplant outcome. Overall survival was not different between patients who received dose reduction, no modification, or escalation of BU (68%, 67%, and 50% at 1 year, respectively). Significantly more grade III–IV toxicities from days 29 to 100 were observed in patients who received dose escalation (Fisher's exact test, $P = 0.023$) (Table S2). No difference in TRM was observed among these three groups.

All three patients who developed early-onset SOS within 20 days after transplant had received dose reduction of BU. Two developed grade II liver toxicity, and another developed grade IV liver toxicity before day 28 (Fig. 4b). Two patients who had late-onset SOS and died had received dose escalation (Fig. 4c).
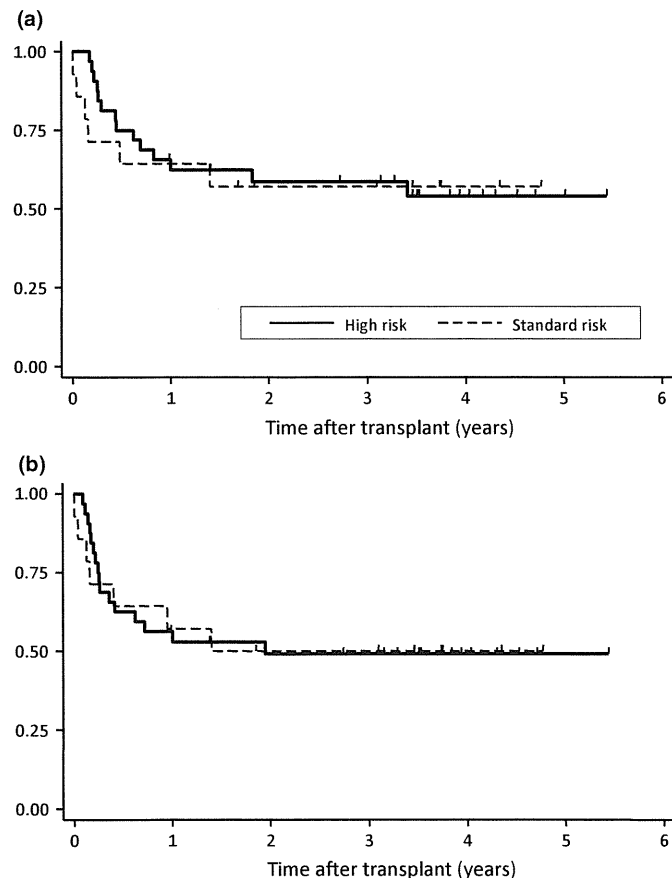
(a)

(b)

Fig. 2. Overall survival and disease-free survival curves according to disease risk in patients receiving allogeneic hematopoietic stem cell transplantation treated with targeted oral busulfan and cyclophosphamide. Overall survival (a) and disease-free survival (b), each stratified according to disease risk. Data were analyzed with the Kaplan–Meier method.
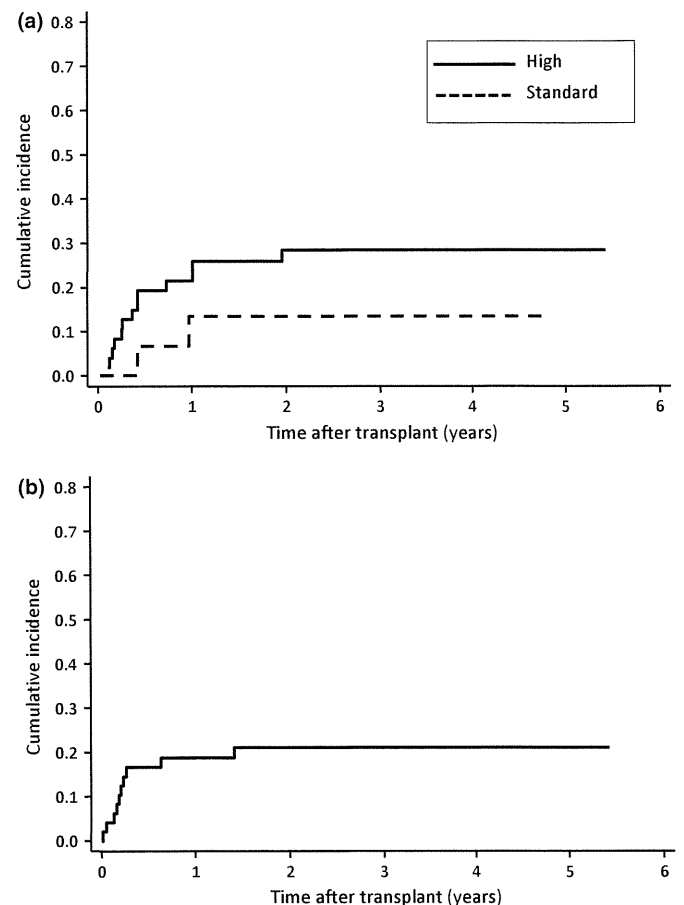
(a)

(b)

Fig. 3. Cumulative incidence of relapse and transplant-related mortality in patients receiving allogeneic hematopoietic stem cell transplantation treated with targeted oral busulfan and cyclophosphamide. Cumulative incidence of relapse with (a) high risk disease (22% at 1 year), standard risk disease (14%), and (b) cumulative incidence of treatment-related mortality (18%).
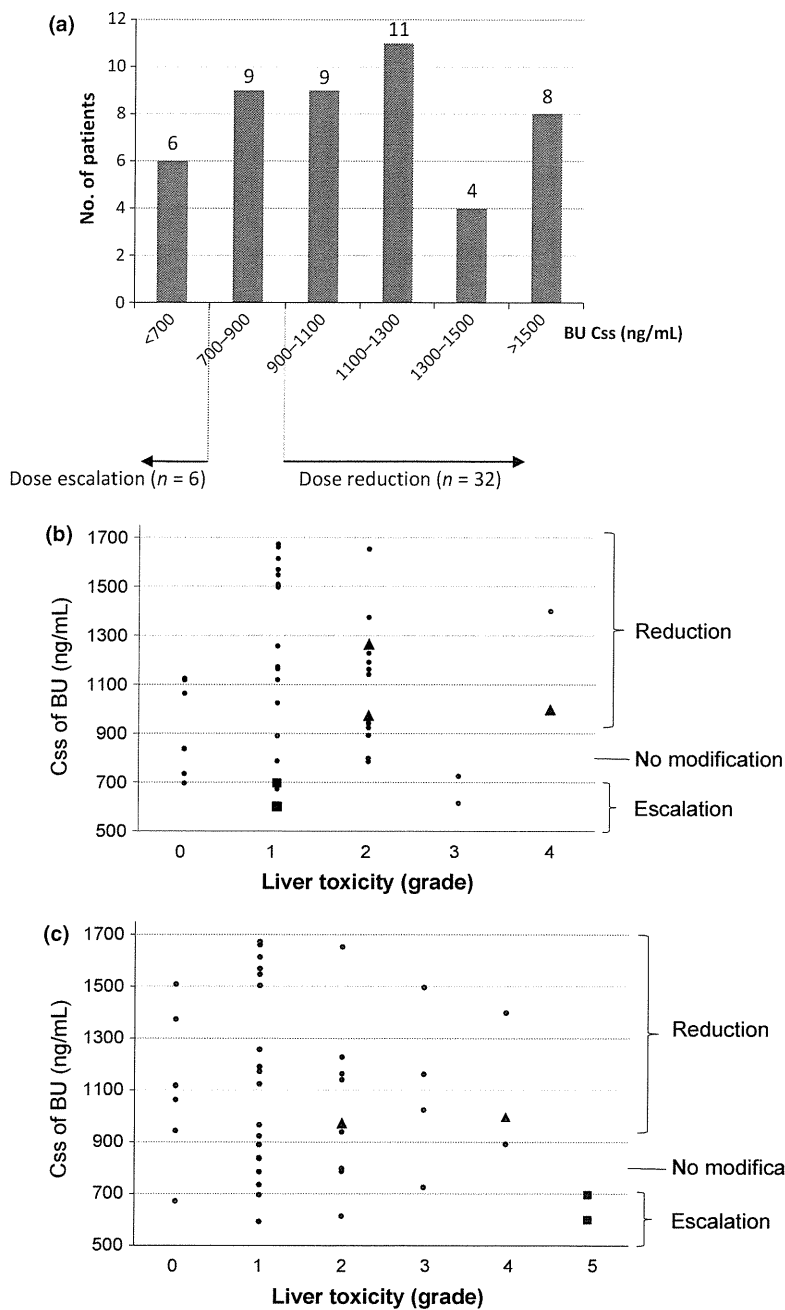
(a)

No. of patients

12
10
8
6
4
2
0

6 · 9 · 9 · 11 · 4 · 8

<700 · 700–900 · 900–1100 · 1100–1300 · 1300–1500 · >1500

BU Css (ng/mL)

Dose escalation (n = 6)   Dose reduction (n = 32)

(b)

Css of BU (ng/mL)

1700
1500
1300
1100
900
700
500

0 1 2 3 4

Liver toxicity (grade)

Reduction

No modification

Escalation

(c)

Css of BU (ng/mL)

1700
1500
1300
1100
900
700
500

0 1 2 3 4 5

Liver toxicity (grade)

Reduction

No modification

Escalation

Fig. 4. Pharmacokinetic studies of busulfin (BU) in patients receiving allogeneic hematopoietic stem cell transplantation. (a) Number of the patients reaching concentration at steady state (Css) with the first BU dose. Six patients received dose escalation, nine patients received no modification, and 32 patients received dose reduction. (b) Liver toxicity in the first 28 days, sinusoidal obstruction syndrome (SOS), and BU dose modification. Triangles (▲) indicate patients diagnosed with SOS before day 20. Two of these patients developed grade II liver toxicity, and another developed grade IV liver toxicity. Two of these patients with early onset SOS died of an unrelated cause. Squares (■) indicate two patients who developed grade I liver toxicity in the first 28 days and were later diagnosed with severe late-onset SOS. (c) Liver toxicity from days 29 to 100, SOS and BU dose modification. Triangles (▲) and squares (■) indicate the same patients as (b). Two patients who had late-onset SOS and died had received dose escalation.

Discussion

We carried out a phase II study of individualizing the oral BU and CY conditioning regimen for adult allogeneic HSCT for myeloid malignancies. In the current study, 1-year OS (65%; 95% CI, 50–77%) clearly exceeded the threshold level of 40%.

Oral administration of BU had been associated with erratic gastrointestinal absorption and resulted in unpredictable systemic drug exposure.[3–5,17] Pharmacokinetic studies of BU and subsequent dose adjustment strategies for the BU and CY conditioning regimen have been reported, mainly among pediatric patients.[18–22] Although no essential difference in PK analysis has been reported between data from Japan and North America,[23] survival data and information on the benefit of the tBU+CY regimen for Asian adult populations are limited.[7] In this phase II study to target the BU Css range of 700

–900 ng/mL, 32 patients received BU dose reduction and the median dose of total BU was reduced. Nevertheless, no increase in relapse was observed and the incidence of TRM was comparable to the BU+CY regimen using the i.v. form.[23] Notably, the incidence of SOS (11% at day 100) was relatively lower than in the previous report of an adult population receiving the CY+total body irradiation regimen[24] or oral non-targeted BU+CY.[6] Severe SOS was not observed within 20 days after transplantation, and this targeting strategy may contribute to reduce the severity of early-onset SOS. Our positive results could be a consequence of adjusting the BU dose, considering that 38 of 47 patients (81%) actually had not achieved optimal Css after the first dose. That is, the fixed dose of BU was not optimal in 81% of these Japanese patients.

In our previous study, SOS was not observed among patients whose Css range was within the target dose or when the BU dose

- 38 -

was reduced (Akio Kohno, Mariko Fukumoto, Hiroto Narimatsu, Kazutaka Ozeki, Masashi Sawa, Shuichi Mizuta, Hitoshi Suzuki, Isamu Sugiura, Seitaro Terakura, Kazuko Kudo, and Yoshihisa Morishita, unpublished data, 2003). In the current study, three patients in the BU reduction group developed early-onset SOS, although the estimated cumulative Css remained within the targeted range. Liver toxicity in these patients might also be related to increased exposure to toxic metabolites of CY.[24] A dose-escalation study using test dose PK also showed that patients who showed a high level of AUC in the first dose developed severe toxicity, including hepatic SOS.[25]

Two of the six patients who received dose escalation experienced late-onset severe SOS. We may need to be cautious of possible late-onset severe SOS after dose escalation of BU. However, the causal relationship between dose escalation of BU based on low initial Css and SOS needs to be further evaluated, because individual oral BU PK are influenced by many factors. Glutathione S-transferase-mediated conjugation with GSH is the main mechanism to detoxify BU. Accumulation of the active metabolite of CY through depletion of the cellular GSH pool may contribute hepatic toxicity.[26] Hepatic GST activity and GST gene polymorphisms have been shown to be associated with BU clearance as well as transplant outcome. Polymorphism of GSTM1 is reported as a risk factor of SOS.[27] The heterozygous variant of GSTA1 (GSTA1*A/*B), which is observed in 26% of the Japanese population, resulted in slower elimination of BU than the wild-type.[28] Analysis using the Japan Marrow Donor Program showed a higher risk of TRM among recipients with the GSTM1-positive genotype, which was different from the Caucasian population.[29] We are currently investigating gene polymorphisms reported to be related with the risk factors of transplantation, such as GST genes and the UDP glucosyltransferase gene family[30] in a prospective trial.

Dose targeting possibly improves the OS by alleviating the variable absorptive characteristics among individuals. However, our results also suggest that dose modification might increase the chance of toxicity after day 28, especially in the case of dose escalation, although we should be careful of this interpretation. Dose reduction could generally lead to rejection of the graft. However, in this study, only one patient had 3 days' delay of engraftment in spite of the large number of patients in the study who received a dose reduction of BU. Busulfan in i.v. form has enabled us to accomplish narrow-ranged dose adjustment.[31] Careful validation of the clinical efficacy of PK-based targeting using i.v. BU is warranted.

In conclusion, individual dose adjustment based on BU PK was feasible and effective in the current phase II study.

Acknowledgments

Disclosure Statement

The authors have no conflicts of interest.

Abbreviations

aGVHD	acute graft versus host disease
AUC	area under the blood concentration time curve
BU	busulfan
cGVHD	chronic graft versus host disease
CI	cumulative incidence
Css	concentration at steady state
CY	cyclophosphamide
DFS	disease-free survival
GSH	glutathione
GVHD	graft versus host disease
HLA	human leukocyte antigen
HSCT	hematopoietic stem cell transplantation
LSM	limited sample model
MDS	myelodysplastic syndrome
OS	overall survival
PK	pharmacokinetic
SOS	sinusoidal obstruction syndrome
tBU+CY	targeting BU+CY
TRM	transplant-related mortality

References

1 Tutschka PJ, Copelan EA, Klein JP. Bone marrow transplantation for leukemia following a new busulfan and cyclophosphamide regimen. *Blood* 1987; **70**: 1382–8.

2 Socie G, Clift RA, Blaise D *et al.* Busulfan plus cyclophosphamide compared with total-body irradiation plus cyclophosphamide before marrow transplantation for myeloid leukemia: long-term follow-up of 4 randomized studies. *Blood* 2001; **98**: 3569–74.

3 Slattery JT, Clift RA, Buckner CD *et al.* Marrow transplantation for chronic myeloid leukemia: the influence of plasma busulfan levels on the outcome of transplantation. *Blood* 1997; **89**: 3055–60.

4 Dix SP, Wingard JR, Mullins RE *et al.* Association of busulfan area under the curve with veno-occlusive disease following BMT. *Bone Marrow Transplant* 1996; **17**: 225–30.

5 Vassal G, Deroussent A, Hartmann O *et al.* Dose-dependent neurotoxicity of high-dose busulfan in children: a clinical and pharmacological study. *Cancer Res* 1990; **50**: 6203–7.

6 Kashyap A, Wingard J, Cagnoni P *et al.* Intravenous versus oral busulfan as part of a busulfan/cyclophosphamide preparative regimen for allogeneic hematopoietic stem cell transplantation: decreased incidence of hepatic venoocclusive disease (HVOD), HVOD-related mortality, and overall 100-day mortality. *Biol Blood Marrow Transplant* 2002; **8**: 493–500.

7 Takamatsu Y, Sasaki N, Eto T *et al.* Individual dose adjustment of oral busulfan using a test dose in hematopoietic stem cell transplantation. *Int J Hematol* 2007; **86**: 261–8.

8 Fukumoto M, Kubo H, Ogamo A. Quantitative determination of busulfan in serum using gas chromatography - Mass spectrometry in negative-ion chemical ionization mode. *Anal Lett* 2001; **34**: 761–71.

9 Grochow LB, Jones RJ, Brundrett RB *et al.* Pharmacokinetics of busulfan: correlation with veno-occlusive disease in patients undergoing bone marrow transplantation. *Cancer Chemother Pharmacol* 1989; **25**: 55–61.

10 Terakura S, Atsuta Y, Sawa M *et al.* A prospective dose-finding trial using a modified continual reassessment method for optimization of fludarabine plus melphalan conditioning for marrow transplantation from unrelated donors in patients with hematopoietic malignancies. *Ann Oncol* 2011; **22**: 1865–71.

11 Deeg HJ, Lin D, Leisenring W *et al.* Cyclosporine or cyclosporine plus methylprednisolone for prophylaxis of graft-versus-host disease: a prospective, randomized trial. *Blood* 1997; **89**: 3880–7.

12 McDonald GB, Hinds MS, Fisher LD *et al.* Veno-occlusive disease of the liver and multiorgan failure after bone marrow transplantation: a cohort study of 355 patients. *Ann Intern Med* 1993; **118**: 255–67.

13 Jones RJ, Lee KS, Beschorner WE *et al.* Venoocclusive disease of the liver following bone marrow transplantation. *Transplantation* 1987; **44**: 778–83.

14 Shulman HM, Hinterberger W. Hepatic veno-occlusive disease–liver toxicity syndrome after bone marrow transplantation. *Bone Marrow Transplant* 1992; **10**: 197–214.

15 Cheson BD, Cassileth PA, Head DR *et al.* Report of the National Cancer Institute-sponsored workshop on definitions of diagnosis and response in acute myeloid leukemia. *J Clin Oncol* 1990; **8**: 813–9.

16 Kolb HJ. Management of relapse after hematopoietic cell transplantation. In: Thomas EDBK, Forman SJ, eds. *Hematopoietic Cell Transplantation*, 2nd edn. Boston, MA: Blackwell Science, 1999; 929–36.

17 Grochow LB. Busulfan disposition: the role of therapeutic monitoring in bone marrow transplantation induction regimens. *Semin Oncol* 1993; **20**: 18–25; quiz 26.

18 Bolinger AM, Zangwill AB, Slattery JT *et al.* Target dose adjustment of busulfan in pediatric patients undergoing bone marrow transplantation. *Bone Marrow Transplant* 2001; **28**: 1013–8.

19 Brice K, Valerie B, Claire G *et al.* Risk-adjusted monitoring of veno-occlusive disease following Bayesian individualization of busulfan dosage for bone marrow transplantation in paediatrics. *Pharmacoepidemiol Drug Saf* 2008; **17**: 135–43.

20 Tran H, Petropoulos D, Worth L *et al.* Pharmacokinetics and individualized dose adjustment of intravenous busulfan in children with advanced hematologic malignancies undergoing allogeneic stem cell transplantation. *Biol Blood Marrow Transplant* 2004; **10**: 805–12.

21 Dupuis LL, Sibbald C, Schechter T *et al.* IV busulfan dose individualization in children undergoing hematopoietic stem cell transplant: limited sampling strategies. *Biol Blood Marrow Transplant* 2008; **14**: 576–82.

22 Zwaveling J, Bredius RG, Cremers SC *et al.* Intravenous busulfan in children prior to stem cell transplantation: study of pharmacokinetics in association with early clinical outcome and toxicity. *Bone Marrow Transplant* 2005; **35**: 17–23.

23 Kim SW, Mori SI, Tanosaki R *et al.* Busulfex (i.v. BU) and CY regimen before SCT: Japanese-targeted phase II pharmacokinetics combined study. *Bone Marrow Transplant* 2009; **43**: 611–7.

24 McDonald GB, Slattery JT, Bouvier ME *et al.* Cyclophosphamide metabolism, liver toxicity, and mortality following hematopoietic stem cell transplantation. *Blood* 2003; **101**: 2043–8.

25 O'Donnell PH, Artz AS, Undevia SD *et al.* Phase I study of dose-escalated busulfan with fludarabine and alemtuzumab as conditioning for allogeneic

26 Hassan M, Ljungman P, Ringden O *et al.* The effect of busulphan on the pharmacokinetics of cyclophosphamide and its 4-hydroxy metabolite: time interval influence on therapeutic efficacy and therapy-related toxicity. *Bone Marrow Transplant* 2000; **25**: 915–24.

27 Srivastava A, Poonkuzhali B, Shaji RV *et al.* Glutathione S-transferase M1 polymorphism: a risk factor for hepatic venoocclusive disease in bone marrow transplantation. *Blood* 2004; **104**: 1574–7.

28 Kusama M, Kubota T, Matsukura Y *et al.* Influence of glutathione S-transferase A1 polymorphism on the pharmacokinetics of busulfan. *Clin Chim Acta* 2006; **368**: 93–8.

29 Terakura S, Murata M, Nishida T *et al.* Increased risk for treatment-related mortality after bone marrow transplantation in GSTM1-positive recipients. *Bone Marrow Transplant* 2006; **37**: 381–6.

30 Terakura S, Murata M, Nishida T *et al.* A UGT2B17-positive donor is a risk factor for higher transplant-related mortality and lower survival after bone marrow transplantation. *Br J Haematol* 2005; **129**: 221–8.

31 Pidala J, Kim J, Anasetti C *et al.* Targeted i.v. BU and fludarabine (t-i.v. BU/Flu) provides effective control of AML in adults with reduced toxicity. *Bone Marrow Transplant* 2011; **46**: 641–9.

Supporting Information

Additional Supporting Information may be found in the online version of this article:

Fig. S1. Study scheme.

Table S1. Regimen-related toxicity before day 28 in patients receiving allogeneic hematopoietic stem cell transplantation treated with targeted oral busulfan and cyclophosphamide.

Table S2. Regimen-related toxicity (day 29–100) in patients receiving allogeneic hematopoietic stem cell transplantation treated with targeted oral busulfan and cyclophosphamide.

Please note: Wiley-Blackwell are not responsible for the content or functionality of any supporting materials supplied by the authors. Any queries (other than missing material) should be directed to the corresponding author for the article.

Cellular Immunology
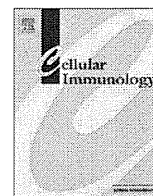
Escape of leukemia blasts from HLA-specific CTL pressure in a recipient of HLA one locus-mismatched bone marrow transplantation

Tomonori Kato [1], Seitaro Terakura [1], Makoto Murata *, Kyoko Sugimoto, Miho Murase, Chisako Iriyama, Akihiro Tomita, Akihiro Abe, Momoko Suzuki, Tetsuya Nishida, Tomoki Naoe

Department of Hematology and Oncology, Nagoya University Graduate School of Medicine, 65 Tsurumai-cho, Showa-ku, Nagoya, Aichi 466-8550, Japan

ABSTRACT

A case of leukemia escape from an HLA-specific cytotoxic T lymphocyte (CTL) response in a recipient of bone marrow transplantation is presented. Only the expression of HLA-B51, which was a mismatched HLA locus in the graft-versus-host direction, was down-regulated in post-transplant leukemia blasts compared with that in pre-transplant blasts. All CTL clones, that were isolated from the recipient's blood when acute graft-versus-host disease developed, recognized the mismatched B*51:01 molecule in a peptide-dependent manner. The pre-transplant leukemia blasts were lysed by CTL clones, whereas the post-transplant leukemia blasts were not lysed by any CTL clones. The IFN-γ ELISPOT assay revealed that B*51:01-reactive T lymphocytes accounted for the majority of the total alloreactive T lymphocytes in the blood just before leukemia relapse. These data suggest that immune escape of leukemia blasts from CTL pressure toward a certain HLA molecule can lead to clinical relapse after bone marrow transplantation.

© 2012 Elsevier Inc. All rights reserved.

1. Introduction

Allogeneic hematopoietic stem cell transplantation (HSCT) is curative for leukemia by virtue of the immune reaction mediated by donor T lymphocytes, termed the graft-versus-leukemia (GVL) effect [1]. For HSCT recipients from HLA-matched donors, the GVL effect can be triggered by minor histocompatibility antigens [2–4], and several studies using sequential flow cytometric analysis with tetramers have clearly demonstrated that minor histocompatibility antigen-specific T lymphocytes increase in frequency in the recipient's blood before and during clinical regression of leukemia [5–10]. On the other hand, for HLA-mismatched HSCT recipients, extremely limited biological studies have demonstrated that the GVL effect can be mediated by mismatched HLA-specific donor T lymphocytes [11].

Allogeneic HSCT is a well-established immunotherapy for leukemia, but, unfortunately, some recipients relapse after transplantation. It is difficult to evaluate the role of individual factors in relapse. Nevertheless, it is reasonable to assume that the selective pressure exerted by donor T lymphocytes can lead to the outgrowth of pre-existing leukemia variants that have lost expression of gene products such as HLA molecules. Some studies have demonstrated loss of the mismatched HLA haplotype in the

leukemia blasts of HSCT recipients as a consequence of loss of heterozygosity in chromosome 6 [12–14]. However, the mechanisms involved in leukemia relapse after HLA locus-mismatched HSCT remain largely uninvestigated.

This paper presents a case of selective HLA down-regulation in post-transplant leukemia blasts but not in pre-transplant blasts of a recipient who received bone marrow transplantation from an HLA one locus-mismatched donor. All cytotoxic T lymphocyte (CTL) clones that were isolated from the recipient's blood during acute graft-versus-host disease (GVHD) demonstrated cytotoxicity specific for the mismatched HLA-B molecule, lysed pre-transplant blasts but not post-transplant blasts, and persisted in the patient's blood until leukemia relapse. These results suggest that immune escape of leukemia blasts from CTL pressure toward a certain HLA allele can lead to clinical relapse.

2. Patient, materials and methods

2.1. Patient

A 24-year-old man with primary refractory T lymphoblastic leukemia/lymphoma received allogeneic bone marrow transplantation without ex vivo T lymphocyte depletion from his mother. Because the patient had neither a sibling nor an HLA-matched unrelated donor, his mother was chosen as an alternative donor. PCR sequencing-based typing for HLA alleles of the patient and mother revealed one HLA-B allele mismatch in

---

* Corresponding author. Fax: +81 52 744 2157.
 E-mail address: mmurata@med.nagoya-u.ac.jp (M. Murata).
 [1] These authors contributed equally.

Table 1
HLA types of the patient and donor.

	A	B	C	DRB1	DQB1	DPB1
Patient	1101/2402	5401/<u>5101</u>	0102/–	0901/–	0303/–	0501/–
Donor	1101/2402	5401/5201	0102/1202	0901/1502	0303/0601	0501/–

The mismatched HLA allele in the graft-versus-host direction is underlined.

the graft-versus-host direction (Table 1). The preparative regimen consisted of 180 mg/m^2 melphalan and 12 Gy total body irradiation. GVHD prophylaxis consisted of 0.03 mg/kg tacrolimus and short-term methotrexate. Neutrophil engraftment (neutrophil count $\geqslant 0.5 \times 10^9$/l) was achieved 14 days after transplantation with full donor-type chimera. The patient developed severe acute GVHD involving the skin, gut, and liver on day 46 (maximum stage: skin 3, gut 2, and liver 1; maximum grade: III on day 53), evaluated according to previously published criteria [15]. Acute GVHD was temporarily controlled by additional immunosuppressants, but it was incurable and transitioned to chronic GVHD. On day 261, the patient relapsed with ascites, a hydrocele, and a subpapillary tumor. Leukemia blasts in the ascites fluid were confirmed by cytological examination. Immunosuppressant therapy was required to control GVHD until his death on day 279.

2.2. Cell culture

CTL clones were isolated from a blood sample as described previously [16]. Briefly, peripheral blood mononuclear cells (PBMCs) obtained from the recipient on day 56, when severe acute GVHD developed, were stimulated in vitro with aliquots of γ-irradiated PBMCs that had been obtained from the recipient pre-transplant and cryopreserved. After three weekly stimulations, the CTL clones were isolated from the polyclonal T lymphocyte culture by limiting dilution. The CTLs were expanded by stimulation every 14 days with 30 ng/ml OKT3 monoclonal antibody (Janssen Pharmaceutical), using unrelated allogeneic γ-irradiated (25 Gy) PBMCs and γ-irradiated (75 Gy) EB virus-transformed lymphoblastoid cells (B-LCL) as feeder cells. The culture medium consisted of RPMI-1640-HEPES (Sigma–Aldrich) containing 10% pooled, heat-inactivated human serum, and recombinant human IL-2 (R&D Systems). The T lymphocytes were used in assays 14 days after stimulation or 1 day after thawing of a frozen aliquot. All samples were collected after written informed consent had been obtained. B-LCLs were maintained in RPMI-1640-HEPES with 10% FBS. COS cells were maintained in DMEM (Sigma–Aldrich) with 10% FBS.

2.3. Flow cytometric analysis

Leukemia blasts were incubated at 37 °C for 30 min with anti-HLA-A24/A23 (One lambda), anti-HLA-A11/A1/A26 (One lambda), and anti-HLA-B51/B52/B49/B56 (One lambda) antibodies to detect A24, A11, and B51, respectively, of patient cells followed by incubation at 37 °C for 15 min with fluorescein isothiocyanate-conjugated antimouse IgM (Beckman Coulter). To detect HLA-DR9 of patient cells, leukemia blasts were incubated at 37 °C for 30 min with fluorescein isothiocyanate-conjugated anti-HLA-DR antibody (BD Pharmingen). Antibody to detect HLA-B54 without cross-reaction to B51 was not available. After washing, the cells were analyzed by a BD FACSAria (BD Biosciences). Leukemia blasts were sorted by BD FACSAria with anti-CD7 (BD Biosciences) and anti-CD10 (eBiosciences) antibodies from pre-transplant bone marrow and post-transplant ascites fluid samples. The purities of pre-transplant and post-transplant blasts were ∼62% and ∼99%, respectively. CTL clones were analyzed using three-color flow cytometry for expression of CD3,

CD4, and CD8 using phycoerythrin-cyanin 5.1-conjugated anti-CD3 (Beckman Coulter), phycoerythrin-conjugated anti-CD4 (BD Biosciences), and fluorescein isothiocyanate-conjugated anti-CD8 (BD Biosciences) antibodies.

2.4. Chromium release assay

Leukemia blasts and B-LCLs were used as target cells in a cytotoxicity assay. Leukemia blasts and B-LCLs were labeled for 2 h with ^{51}Cr. After washing, the cells were dispensed at 2×10^3 cells/well into triplicate cultures in 96-well plates and incubated for 4 h at 37 °C with CTL clones at various E:T ratios. Percent-specific lysis was calculated as [(experimental cpm − spontaneous cpm)/(maximum cpm − spontaneous cpm)] ×100.

2.5. Determination of T cell receptor (TCR)-Vβ gene usage and nucleotide sequences

TCR Vβ usage was assessed by RT-PCR using primers covering the entire families of functional TCR Vβ chains [17–19]. Briefly, total RNA was extracted from individual CTL clones, and cDNA was synthesized using SuperScript III RT (Invitrogen). RT-PCR reactions were carried out with the appropriate Vβ sense primers specific for different Vβ families and a primer specific for the constant region of TCR-β. Subsequently, the complementarity determining region 3(CDR3) of each positive PCR product was sequenced with corresponding antisense primer. TCR Vβ gene usage was determined by the international ImMunoGeneTics information system (IMGT) software, IMGT/V-QUEST (http://www.imgt.org/).

2.6. HLA-B cDNA constructs

Total RNA was extracted from the patient and donor B-LCLs and converted into cDNA. Constructs containing the full-length HLA-B*51:01, B*52:01, and B*54:01 cDNA were generated from the cDNA by PCR and cloned into the pEAK10 expression vector (Edge Bio-Systems). Two mutated HLA-B*51:01 cDNA constructs, in which amino acid at position 63 or 67 was substituted with the corresponding amino acid in B*52:01, and two more mutated HLA-B*51:01 cDNA constructs, in which the amino acid at position 194 or 199 was substituted with the corresponding amino acid in B*44:03, were produced using the QuikChange Site-Directed Mutagenesis Kit (Stratagene).

2.7. Transfection of B-LCLs and COS cells with HLA cDNA

B-LCL (5×10^6) were transfected by electroporation (200 V, 500 μFD) in 200 μl of potassium-PBS with the 15 μg of pEAK10 plasmid encoding HLA-B*51:01 cDNA and selected with puromycin (Edge BioSystems), beginning 48 h after transfection. Three days after selection, they were used as targets in a chromium release assay. COS cells (5×10^3) were plated in individual wells of 96-well flat-bottom plates and transfected with 100 ng of the pEAK10 plasmid encoding HLA-B*51:01, HLA-B*52:01, HLA-B*54:01, or mutated HLA-B*51:01 cDNA using the FuGENE 6 Transfection Reagent (Roche).

2.8. CTL stimulation assay

COS transfectants (5×10^3) were cocultured with CTL clones (2×10^4) in individual wells of 96-well flat-bottom plates for 24 h at 37 °C, and IFN-γ production was measured in the supernatant using ELISA (Endogen).

2.9. Enzyme-linked immunospot (ELISPOT) assay

T lymphocytes were isolated from recipient's PBMCs by negative depletion using the Pan T Cell Isolation Kit II (Miltenyi Biotec) and used as responder T cells. Responder T cells at a concentration of 2×10^5 per well were plated in individual wells of the 96-well MultiScreen-IP filter plates (Millipore) coated with anti-human interferon (IFN)-γ antibody (5 μg/ml; Mabtech) and tested in triplicate against a total of 2×10^5 stimulator cells: patient B-LCL, donor B-LCL, and HLA-B*51:01-transfected donor B-LCL. The plates were incubated for 24 h at 37°C, washed, and incubated with biotinylated anti-human IFN-γ antibody (1 μg/ml; Mabtech) for 2 h at room temperature. After addition of streptavidin (Fitzgerald Industries International) to the wells, the plates were developed with a 3-amino-9-ethylcarbazol substrate kit (Vector Laboratories). Spots were counted using a microscope, and mean numbers were calculated from triplicate wells after subtraction of the number of spots obtained with medium alone.

3. Results

3.1. Selective down-regulation of HLA-B locus in post-transplant leukemia blasts

To determine whether expressions of some HLA loci in post-transplant relapsed leukemia blasts were down-regulated or lost, flow cytometric analysis was performed for HLA-A*24:02, A*11:01, B*51:01, and DR*09:01 using anti-HLA-A24/A23, -HLA-A11/A1/A26, -HLA-B51/B52/B49/B56, and -pan HLA-DR antibodies, respectively. The expression of B*51:01 was down-regulated in post-transplant leukemia blasts compared with that in pre-transplant blasts, whereas expressions of A*24:02, A*11:01, and DR*09:01 were the same or higher in post-transplant blasts than in pre-transplant blasts (Fig. 1). These data led us to question whether B*51:01-selective pressure mediated by donor T lymphocytes was present in the patient post-transplant.

3.2. Isolation of alloreactive CTL clones

Ten CTL clones, termed TK1 to TK10, were isolated from the peripheral blood of the recipient during acute GVHD. In a cytotoxicity assay, all isolated clones lysed recipient B-LCL but failed to lyse donor B-LCL (Fig. 2), demonstrating that all clones were alloreactive. Flow cytometric analysis revealed that all CTL clones
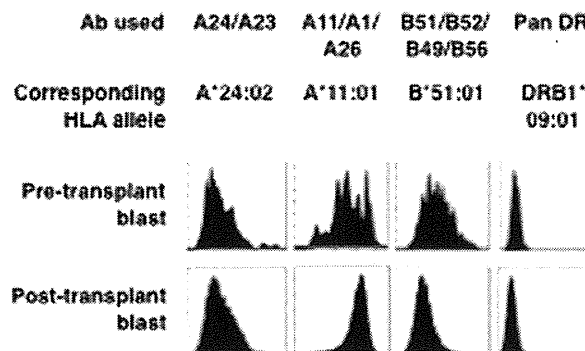

Fig. 1. HLA expression on leukemia blasts. Pre-transplant and post-transplant leukemia blasts were stained with anti-HLA-A24/A23, anti-HLA-A11/A1/A26, anti-HLA-B51/B52/B49/B56, and anti-HLA-pan DR antibodies to detect A*24:02, A*11:01, B*51:01, and DRB1*09:01, respectively. Data are representative of four experiments.
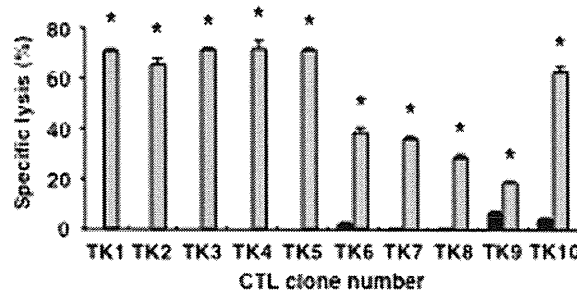

Fig. 2. Cytotoxicities of CTL clones against B-LCLs. B-LCLs that originated from the recipient (gray) and the donor (black) were used as targets for CTL clones. Specific lysis is shown as the mean and SD of triplicate cultures at an E:T ratio of 10:1. *Significant difference ($p < 0.0001$: Student's t-test) in the lysis of recipient B-LCL compared with donor B-LCL. Data are representative of three experiments.

Table 2
Clonotypes of isolated CTL clones.

| CTL	TCR Vβ	Nucleotide and deduced amino acid sequences of complementarity determining region 3															
TK1	Vβ6.5	GCC	AGC	AGT	CCC	GGG	ACT	AGC	GGA	ACC	TAC	GAG	CAG	TAC	TTC		
		A	S	S	P	G	T	S	G	T	Y	E	Q	Y	F		
TK2	Vβ20	AGT	CAG	GGG	CCG	GCG	GTT	ACC	GGG	GAG	CTG	TTT	TTT				
		S	Q	G	P	A	V	T	G	E	L	F	F				
TK3	Vβ20	AGT	CAG	GGG	CCG	GCG	GTT	ACC	GGG	GAG	CTG	TTT	TTT				
		S	Q	G	P	A	V	T	G	E	L	F	F				
TK4	Vβ19*1	GCC	AGT	ACT	TGG	GGT	TAC	CCA	CAG	GGG	CCC	GGT	GCG	GAT	ACC	GGG	GAG	CTG	TTT	TTT
		A	S	T	W	G	Y	P	Q	G	P	G	A	D	T	G	E	L	F	F
TK5	Vβ19*1	GCC	AGT	ACT	TGG	GGT	TAC	CCA	CAG	GGG	CCC	GGT	GCG	GAT	ACC	GGG	GAG	CTG	TTT	TTT
		A	S	T	W	G	Y	P	Q	G	P	G	A	D	T	G	E	L	F	F
TK6	Vβ12	GCC	AGC	AGT	TTA	GCT	AGC	GGG	AGG	GCC	TCC	CAT	GAG	CAG	TTC	TTC		
		A	S	S	L	A	S	G	R	A	S	H	E	Q	F	F		
TK7	Vβ12	GCC	AGC	AGT	TTA	GCT	AGC	GGG	AGG	GCC	TCC	CAT	GAG	CAG	TTC	TTC		
		A	S	S	L	A	S	G	R	A	S	H	E	Q	F	F		
TK8	ND																
TK9	Vβ12	GCC	AGC	AGT	TTA	GCT	AGC	GGG	AGG	GCC	TCC	CAT	GAG	CAG	TTC	TTC		
		A	S	S	L	A	S	G	R	A	S	H	E	Q	F	F		
TK10	Vβ2	GCC	AGC	AGT	GAC	TCT	ATC	GCG	GAT	GAG	CAG	TTC	TTC				
		A	S	S	D	S	I	A	D	E	Q	F	F				

ND, not detected.

A

B
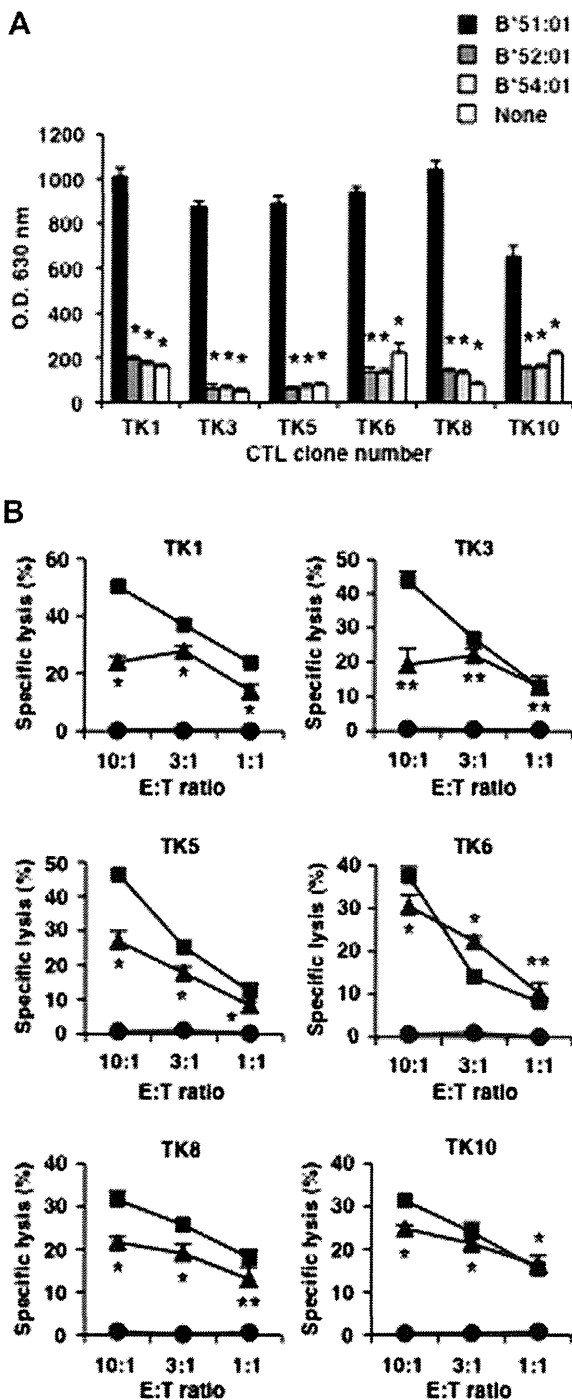
Fig. 3. Recognition of the HLA-B*51:01 molecule by CTLs. (A) COS cells were transfected with a plasmid encoding B*51:01 cDNA, B*52:01 cDNA, B*54:01 cDNA, or no cDNA cocultured with CTL clones, and IFN-γ production was measured in the supernatant using ELISA. Data are the means and SD of triplicate determinations. *Significant difference (p < 0.01: Student's t-test) in the IFN-γ production stimulated by B*52:01 cDNA, B*54:01 cDNA or no cDNA compared with B*51:01 cDNA. Data are representative of three experiments. (B) Recipient B-LCL (square), donor B-LCL (circle), and donor B-LCL transfected with HLA-B*51:01 cDNA (triangle) were used as targets for CTL clones. Specific lysis is shown as the mean and SD of triplicate cultures at various E:T ratios. Significant difference (*p < 0.01; **p < 0.05) in the lysis of B*51:01-transfected donor B-LCL compared with donor B-LCL (negative control). Data are representative of three experiments.

were CD3+/CD4−/CD8+ (data not shown). The nucleotide sequences of the uniquely rearranged TCR Vβ gene of each clone were determined by direct DNA sequencing of the amplified PCR

products of TCR (Table 2). The TK2 and TK3 clones had the same nucleotide sequences in the CDR3 regions of their TCR Vβ20, suggesting that these CTLs originated from a single clone. Similarly, TK4 and TK5, as well as TK6, TK7, and TK9, had the same nucleotide sequences in the CDR3 regions of their TCR Vβ19*1 and Vβ12, respectively, suggesting that each group also originated from a single clone. Thus, the 10 isolated alloreactive CTL clones appeared to have been derived from six independent clones.

3.3. CTL clones recognized the HLA-B*51:01 molecule

To evaluate the possibility that isolated CTL clones recognize the HLA-B*51:01 molecule, COS cells were first transfected with an HLA-B*51:01, −B*52:01, or −B*54:01 cDNA construct, COS transfectants were cocultured with six independent CTL clones, and then the production of IFN-γ in the supernatant was measured. The COS cells transfected with HLA-B*51:01 clearly stimulated IFN-γ production by six independent CTL clones, whereas neither B*52:01 nor B*54:01 stimulated them (Fig. 3A). Then, donor B-LCL were transfected with an HLA-B*51:01 cDNA construct and used as target cells in a cytotoxicity assay. The donor B-LCL transfected with HLA-B*51:01 were lysed by six CTL clones (Fig. 3B), indicating that all clones recognized the mismatched HLA-B*51:01 molecule as an alloantigen. On the other hand, these data suggest that the CTL response toward the HLA-B*51:01 molecule accounted for the majority of the recipient's CTL alloresponse during acute GVHD.

3.4. Recognition of HLA molecules by CTL clones was peptide-dependent

Various forms of T lymphocyte recognition of the allogeneic major histocompatibility antigen, ranging from peptide-dependent to peptide-independent, have been demonstrated [20]. To confirm peptide dependency in CTL recognition, examinations were focused on the difference in the amino acid sequences of the recipient B*51:01 and the donor B*52:01. They differed in two amino acids at positions 63 and 67 (Fig. 4A), which constitute peptide binding pockets A and/or B [21,22]. In particular, B-pocket has a critical role in peptide binding to HLA-B*51:01 molecules [23], and substitution of a single amino acid constituting peptide binding pocket can affect peptide binding [24]. Two mutated B*51:01 cDNA constructs, B*51:01-Asn63Glu and B*51:01-Phe67Ser, in which individual amino acids were substituted with the corresponding amino acid in B*52:01 (Fig. 4A), were generated, as well as two more mutated B*51:01 cDNA constructs, B*51:01-Val194Ile and B*51:01-Ala199Val, in which individual amino acids exist in B*44:02 and other B alleles and localize outside the positions constituting peptide binding pockets. COS cells were then transfected with each wild or mutated cDNA construct and examined in the CTL stimulation assay. IFN-γ production of the TK3 clone was significantly decreased when stimulated by the B*51:01-Phe67Ser mutant in comparison with the wild-type B*51:01 construct (Fig. 4B). IFN-γ production of all other CTL clones, TK1, TK5, TK6, TK8, and TK10, was significantly decreased when stimulated by B*51:01-Asn63Glu and B*51:01-Phe67Ser mutants in comparison with the wild-type B*51:01 construct (Fig. 4B). However, both B*51:01-Val194Ile and B*51:01-Ala199Val mutants stimulated all CTL clones to the same degree as the wild-type B*51:01 construct. Thus, these data suggest that recognition of the HLA-B*51:01 molecule by CTL clones was peptide-dependent.

Furthermore, CTL clones should recognize certain peptides other than leukemia antigens, presented by HLA-B*51:01 molecules, because B*51:01-transfected COS cells, which are derived from monkey kidney cells, stimulated IFN-γ production of CTLs
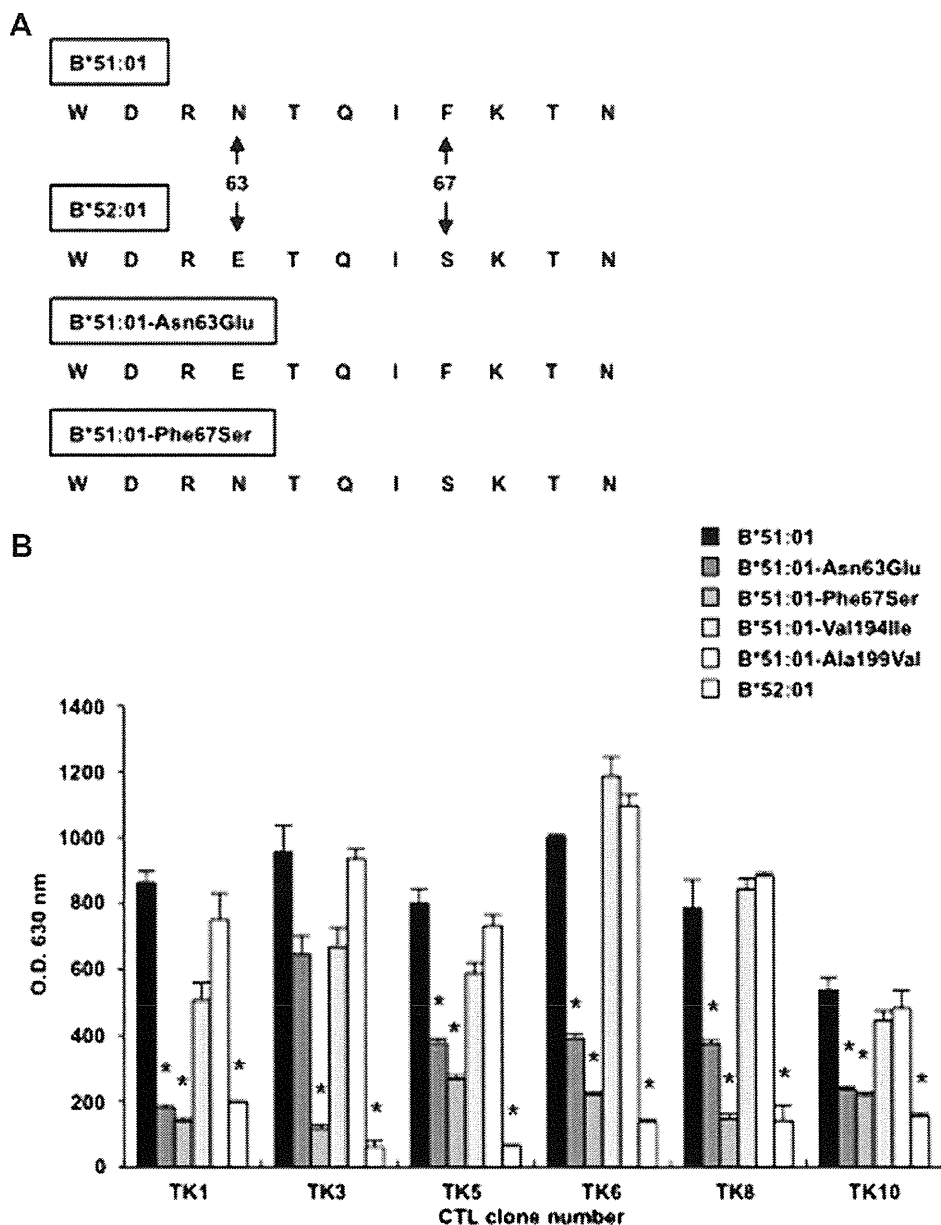
Fig. 4. Recognition of the HLA-B*51:01 molecule by CTLs is peptide-dependent. (A) The amino acid sequences at position 60 to 70 of the B*51:01, B*52:01, B*51:01-Asn63Glu, and B*51:01-Phe67Ser cDNAs are shown. Asn at position 63 was substituted with the corresponding amino acid in B*52:01, Glu, in the B*51:01-Asn63Glu mutant. Phe at position 67 was substituted with the corresponding amino acid in B*52:01, Ser, in the B*51:01-Phe67Ser mutant. (B) COS cells were transfected with a plasmid encoding B*51:01, B*51:01-Asn63Glu, B*51:01-Phe67Ser, B*51:01-Val194Ile, B*51:01-Ala199Val or B*52:01 cDNA construct, cocultured with CTL clones, and IFN-γ production was measured in the supernatant using ELISA. Data are the means and SD of triplicate determinations. *Significant difference (p < 0.05: Student's t-test) in the IFN-γ production stimulated by each mutant or B*52:01 cDNA construct compared with the wild-type B*51:01 cDNA construct. Data are representative of three experiments.

(Fig. 3A), and B*51:01-transfected donor B-LCL, which are derived from B lymphocytes, were lysed by CTLs (Fig. 3B).

3.5. Leukemia blasts escaped from immunological pressure by HLA-B-specific CTLs

Whether the leukemia blasts escaped from the cytotoxicity of HLA-B*51:01-specific CTL clones was then examined. Pre-transplant and post-transplant leukemia blasts were purified by fluorescence-activated cell sorter (purity, ~62% and ~99%, respectively), and a cytotoxicity assay was performed only for the TK1 CTL clone because of the limited number of cryopreserved blasts. Weak but clear lysis of pre-transplant leukemia blasts by the TK1 CTL clone was observed, whereas post-transplant leukemia blasts were not

lysed (Fig. 5A). All other CTL clones (TK3, TK5, TK6, TK8, and TK10) also did not lyse post-transplant leukemia blasts (Fig. 5B).

In addition, whether HLA-B*51:01-specific CTL pressure persisted until leukemia relapse was examined. The IFN-γ ELISPOT assay was performed to detect HLA-B*51:01-reactive CTLs in patient blood on day 232, 1 month before clinical leukemia relapse (Fig. 6). IFN-γ-producing B*51:01-reactive T lymphocytes were detected at a level nearly equal to the level of recipient B-LCL-reactive CTLs, that is, the total CTL alloresponse.

4. Discussion

The mechanism of leukemia relapse in this recipient can be explained as follows. CTLs specific for HLA-B*51:01 molecule/
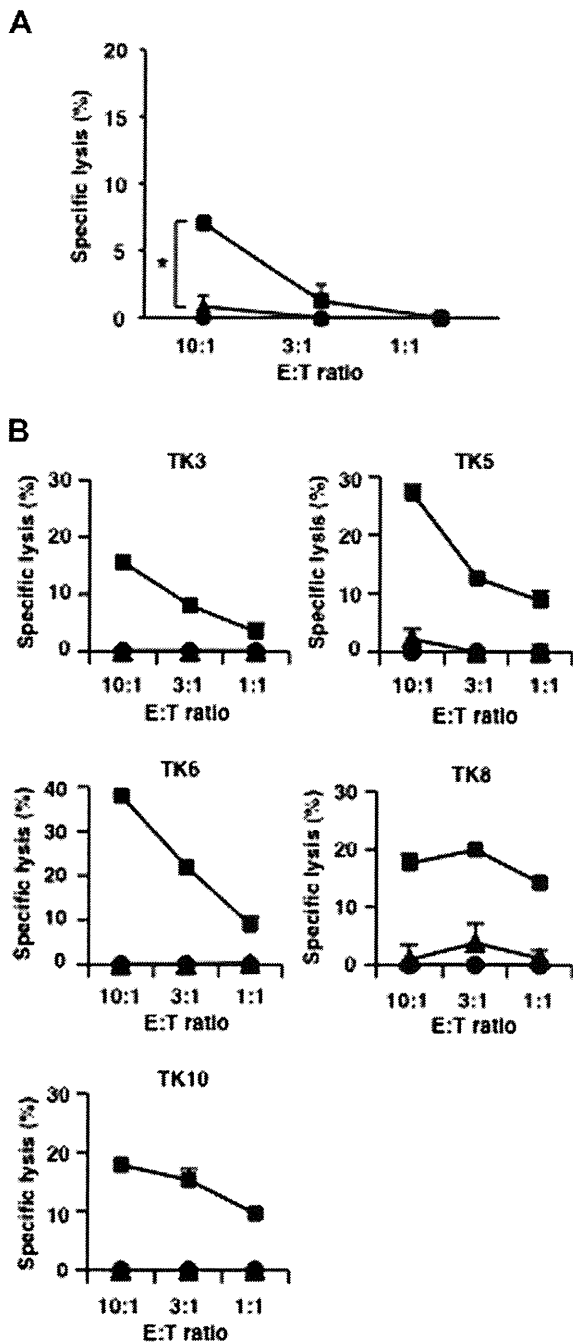
Fig. 5. Cytotoxicities of CTLs against leukemia blasts. (A) Purified pre-transplant leukemia blasts (purity, ~62%) (square), purified post-transplant leukemia blasts (purity, ~99%) (triangle) and donor B-LCL (circle) were used as targets for TK1 CTL clones. Specific lysis is shown as the mean and SD of triplicate cultures at various E:T ratios. *Significant difference (*p* = 0.024: Student's *t*-test) in the lysis of the pre-transplant leukemia blasts compared with the post-transplant leukemia blasts. Data are representative of three experiments. (B) Purified post-transplant leukemia blasts (purity, ~99%) (triangle), B-LCLs from the patient (square) and donor (circle) were used as targets for CTL clones. Specific lysis is shown as the mean and SD of triplicate cultures at various E:T ratios. Data are representative of three experiments. There was no significant difference in the lysis of the post-transplant leukemia blasts compared with B51-negative donor B-LCL (negative control).

Fig. 6. Detection of HLA-B*51:01-specific CTLs in T lymphocytes obtained from the recipient on day 232 after transplantation. (A) Representative ELISPOT wells show triplicate results of T lymphocytes stimulated by recipient B-LCL, donor B-LCL, and *HLA-B*51:01*-transfected donor B-LCL. Data are representative of three experiments. (B) The frequency of CTLs in T lymphocytes recognizing the HLA-B*51:01 molecule was measured by IFN-γ ELISPOT analysis. The frequency of IFN-γ-producing cells is shown against recipient B-LCL (black), donor B-LCL (white), and *HLA-B*51: 01*-transfected donor B-LCL (gray). Data are the means and SD of triplicate determinations. *p = 0.0057; **p = 0.0077; ***p = 0.090 (Student's *t*-test). Data are representative of three experiments.

non-leukemia peptide complex were generated in the recipient blood during acute GVHD, and these CTLs continued to produce immunological pressure on leukemia blasts for at least 8 months after transplantation, but B*51:01-down-regulated leukemia blasts escaped from the pressure of B*51:01-specific CTLs, and then the leukemia clinically relapsed.
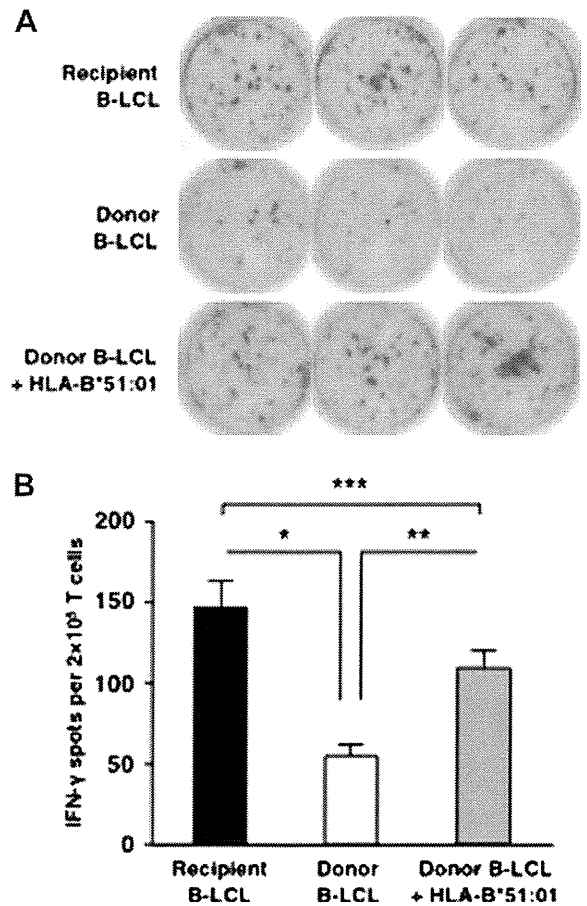
CTLs recognizing mismatched HLA molecules play an important role in the immune reaction after HLA-mismatched HSCT, including graft rejection [25–27], GVHD [28], and the GVL effect [11]. In this study, the mismatched HLA-B*51:01-specific CTLs could participate both in GVHD and the GVL effect in the recipient. Ten CTL clones were isolated from the recipient's blood just after the onset of grade III acute GVHD involving skin, gut, and liver, and all clones demonstrated HLA-B*51:01-specific cytotoxicity in a non-leukemia peptide-dependent manner (Fig. 3 and 4). The patient was suffering from GVHD until his death on day 279, and in the ELISPOT assay for T lymphocytes obtained from recipient blood on day 232, HLA-B*51:01-reactive T lymphocytes accounted for the majority of alloreactive T lymphocytes (Fig. 6). Meanwhile, weak but clear lysis of pre-transplant leukemia blasts by an HLA-B*51:01-specific CTL clone was confirmed (Fig. 5A), and the primary refractory T lymphoblastic leukemia/lymphoma was in remission until day 261. These data are consistent with participation of the recipient HLA-B locus-specific CTLs both in GVHD and the GVL effect.

Selective HLA down-regulation was seen in this patient's post-transplant leukemia blasts. Mechanisms that alter HLA class I expression have been investigated and summarized as follows [29]: (1) loss of heterozygosity in chromosome 6 and/or 15, in

which class I heavy chain or β_2-microglobulin genes are located [30,31]; (2) mutations in these genes [32]; and (3) down-regulation of the antigen processing machinery, including transporter associated with antigen processing and low-molecular-weight protein genes [33]. Ten *HLA-B* cDNAs were cloned from purified post-transplant leukemia blasts (purity, ~99%) by RT-PCR; 5 (50%) clones were identical to the canonical *B*51:01* cDNA sequence, and the others (50%) were identical to the canonical *B*54:01* cDNA sequence, which was another recipient B allele (data not shown). These data suggest that down-regulation of HLA-B*51:01 expression in the post-transplant leukemia blasts resulted from mechanisms other than loss of heterozygosity of B locus and mutation of the *B*51:01* gene itself, although the entire sequence of *B*51:01* DNA including introns has not been determined. Recently, hypermethylation of the HLA-class I gene promoter regions has been identified as a mechanism for transcriptional inactivation of HLA class I genes in esophageal squamous cell carcinoma lesions [34]. We analyzed *B*51:01* promoter methylation by pyrosequencing of bisulfite-treated DNA from purified post-transplant leukemia blasts and confirmed no hypermethylation of the *B*51:01* gene (data not shown). Other possible mechanisms are down-regulation of translation and post-translational modification of the *B*51:01* gene, although, to the best of our knowledge, these mechanisms have not yet been investigated for HLA-class I genes. Further analysis is required.

The change in expression in HLA-A*11:01 between pre-transplant and post-transplant leukemia blasts was of similar magnitude, but in the opposite direction, to that observed for B*51:01. Because the expression of HLA-A11 on target cells can protect them from lysis by KIR3DL2-positive NK cells [35], the possibility that the post-transplant blasts with high expression of HLA-A11 were resistant to NK cell-mediated cytotoxicity, resulting in leukemia relapse, cannot be ruled out.

A question left unresolved is whether the present observation is unique to this recipient or can be duplicated in additional recipients who receive HLA one locus-mismatched HSCT. However, the present findings can explain, at least in part, the mechanism of how leukemia relapse occurs during persistent GVHD after HSCT. Another question is whether the present observation is unique to T lymphoblastic leukemia/lymphoma, which is a relatively rare subset of acute leukemia in adults. The relevance of this finding to other leukemias, including B lymphoblastic leukemia/lymphoma and myeloid malignancies, should be confirmed. Further efforts to identify the peptides that are presented by HLA-B*51:01 molecules and recognized by isolated CTL clones should help to elucidate the precise mechanisms of leukemia escape.

In conclusion, immune escape of leukemia blasts from CTL pressure toward a mismatched HLA molecule/non-leukemia peptide complex may lead to clinical leukemia relapse.

Grant support

Acknowledgment

References

[1] J.H. Antin, Graft-versus-leukemia: no longer an epiphenomenon, Blood 82 (8) (1993) 2273–2277.

[2] E. Goulmy, Human minor histocompatibility antigens: new concepts for marrow transplantation and adoptive immunotherapy, Immunol. Rev. 157 (1997) 125–140.

[3] S.R. Riddell, C. Berger, M. Murata, S. Randolph, E.H. Warren, The graft versus leukemia response after allogeneic hematopoietic stem cell transplantation, Blood Rev. 17 (3) (2003) 153–162.

[4] X. Feng, K.M. Hui, H.M. Younes, A.G. Brickner, Targeting minor histocompatibility antigens in graft versus tumor or graft versus leukemia responses, Trends Immunol. 29 (12) (2008) 624–632.

[5] W.A. Marijt, M.H. Heemskerk, F.M. Kloosterboer, E. Goulmy, M.G. Kester, M.A. van der Hoorn, et al., Hematopoiesis-restricted minor histocompatibility antigens HA-1- or HA-2-specific T cells can induce complete remissions of relapsed leukemia, Proc. Natl. Acad. Sci. USA 100 (5) (2003) 2742–2747.

[6] A. Takami, C. Sugimori, X. Feng, A. Yachie, Y. Kondo, R. Nishimura, et al., Expansion and activation of minor histocompatibility antigen HY-specific T cells associated with graft-versus-leukemia response, Bone Marrow Transplant. 34 (8) (2004) 703–709.

[7] B. de Rijke, A. van Horssen-Zoetbrood, J.M. Beekman, B. Otterud, F. Maas, R. Woestenenk, et al., A frameshift polymorphism in P2X5 elicits an allogeneic cytotoxic T lymphocyte response associated with remission of chronic myeloid leukemia, J. Clin. Invest. 115 (12) (2005) 3506–3516.

[8] E.H. Slager, M.W. Honders, E.D. van der Meijden, S.A. van Luxemburg-Heijs, F.M. Kloosterboer, M.G. Kester, et al., Identification of the angiogenic endothelial-cell growth factor-1/thymidine phosphorylase as a potential target for immunotherapy of cancer, Blood 107 (12) (2006) 4954–4960.

[9] C.A. van Bergen, M.G. Kester, I. Jedema, M.H. Heemskerk, S.A. van Luxemburg-Heijs, F.M. Kloosterboer, et al., Multiple myeloma-reactive T cells recognize an activation-induced minor histocompatibility antigen encoded by the ATP-dependent interferon-responsive (ADIR) gene, Blood 109 (9) (2007) 4089–4096.

[10] T. Nishida, M. Hudecek, A. Kostic, M. Bleakley, E.H. Warren, D. Maloney, et al., Development of tumor-reactive T cells after nonmyeloablative allogeneic hematopoietic stem cell transplant for chronic lymphocytic leukemia, Clin. Cancer Res. 15 (14) (2009) 4759–4768.

[11] D. Montagna, L. Daudt, F. Locatelli, E. Montini, I. Turin, D. Lisini, et al., Single-cell cloning of human, donor-derived antileukemia T-cell lines for in vitro separation of graft-versus-leukemia effect from graft-versus-host reaction, Cancer Res. 66 (14) (2006) 7310–7316.

[12] L. Vago, S.K. Perna, M. Zanussi, B. Mazzi, C. Barlassina, M.T. Stanghellini, et al., Loss of mismatched HLA in leukemia after stem-cell transplantation, N. Engl. J. Med. 361 (5) (2009) 478–488.

[13] I.B. Villalobos, Y. Takahashi, Y. Akatsuka, H. Muramatsu, N. Nishio, A. Hama, et al., Relapse of leukemia with loss of mismatched HLA resulting from uniparental disomy after haploidentical hematopoietic stem cell transplantation, Blood 115 (15) (2010) 3158–3161.

[14] M. Waterhouse, D. Pfeifer, M. Pantic, F. Emmerich, H. Bertz, J. Finke, Genome-wide profiling in AML patients relapsing after allogeneic hematopoietic cell transplantation, Biol. Blood Marrow Transplant. 17 (10) (2011) 1450–1459.

[15] D. Przepiorka, D. Weisdorf, P. Martin, H.G. Klingemann, P. Beatty, J. Hows, et al., 1994 Consensus conference on acute GVHD grading, Bone Marrow Transplant. 15 (6) (1995) 825–828.

[16] M. Murata, E.H. Warren, S.R. Riddell, A human minor histocompatibility antigen resulting from differential expression due to a gene deletion, J. Exp. Med. 197 (10) (2003) 1279–1289.

[17] I. Puisieux, J. Even, C. Pannetier, F. Jotereau, M. Favrot, P. Kourilsky, Oligoclonality of tumor-infiltrating lymphocytes from human melanomas, J. Immunol. 153 (6) (1994) 2807–2818.

[18] L. Garderet, N. Dulphy, C. Douay, N. Chalumeau, V. Schaeffer, M.T. Zilber, et al., The umbilical cord blood alphabeta T-cell repertoire: characteristics of a polyclonal and naive but completely formed repertoire, Blood 91 (1) (1998) 340–346.

[19] G. Folch, M.P. Lefranc, The human T cell receptor beta variable (TRBV) genes, Exp. Clin. Immunogenet. 17 (1) (2000) 42–54.

[20] A. Whitelegg, L.D. Barber, The structural basis of T-cell allorecognition, Tissue Antigens 63 (2004) 101–108.

[21] G.E. Steven, P. Peter, D.B. Linda, The HLA Facts Book, Academic Press, London, 2000 (pp. 52–56).

[22] B. Zhao, A.E. Png, E.C. Ren, P.R. Kolatkar, V.S. Mathura, M.K. Sakharkar, et al., Compression of functional space in HLA-A sequence diversity, Hum. Immunol. 64 (2003) 718–728.

[23] K. Falk, O. Rötzschke, M. Takiguchi, V. Gnau, S. Stevanović, G. Jung, et al., Peptide motifs of HLA-B51, -B52 and -B78 molecules, and implications for Behćet's disease, Int. Immunol. 7 (2) (1995) 223–228.

[24] A. Kikuchi, T. Sakaguchi, K. Miwa, Y. Takamiya, H.G. Rammensee, Y. Kaneko, et al., Binding of nonamer peptides to three HLA-B51 molecules which differ by a single amino acid substitution in the A-pocket, Immunogenetics 43 (5) (1996) 268–276.

[25] J. Pei, Y. Akatsuka, C. Anasetti, M.T. Lin, E.W. Petersdorf, J.A. Hansen, et al., Generation of HLA-C-specific cytotoxic T cells in association with marrow graft rejection: analysis of alloimmunity by T-cell cloning and testing of T-cell-

receptor rearrangements, Biol. Blood Marrow Transplant. 7 (7) (2001) 378–383.

[26] A.B. Kraus, J. Shaffer, H.C. Toh, F. Preffer, D. Dombkowski, S. Saidman, et al., Early host CD8 T-cell recovery and sensitized anti-donor interleukin-2-producing and cytotoxic T-cell responses associated with marrow graft rejection following nonmyeloablative allogeneic bone marrow transplantation, Exp. Hematol. 31 (7) (2003) 609–621.

[27] H. Narimatsu, M. Murata, S. Terakura, K. Sugimoto, T. Naoe, Potential role of a mismatched HLA-specific CTL clone developed pre-transplant in graft rejection following cord blood transplantation, Biol. Blood Marrow Transplant. 14 (4) (2008) 397–402.

[28] K. Sugimoto, M. Murata, S. Terakura, T. Naoe, CTL clones isolated from an HLA-Cw-mismatched bone marrow transplant recipient with acute graft-versus-host disease, J. Immunol. 183 (9) (2009) 5991–5998.

[29] F. Garrido, I. Algarra, A.M. García-Lora, The escape of cancer from T lymphocytes: immunoselection of MHC class I loss variants harboring structural-irreversible "hard" lesions, Cancer Immunol. Immunother. 59 (10) (2010) 1601–1606.

[30] I. Maleno, M.A. López-Nevot, T. Cabrera, J. Salinero, F. Garrido, Multiple mechanisms generate HLA class I altered phenotypes in laryngeal carcinomas: high frequency of HLA haplotype loss associated with loss of heterozygosity in

chromosome region 6p21, Cancer Immunol. Immunother. 51 (7) (2002) 389–396.

[31] T. Rodriguez, R. Méndez, C.H. Roberts, F. Ruiz-Cabello, I.A. Dodi, M.A. López Nevot, et al., High frequency of homozygosity of the HLA region in melanoma cell lines reveals a pattern compatible with extensive loss of heterozygosity, Cancer Immunol. Immunother. 54 (2) (2005) 141–148.

[32] B. Pérez, R. Benitez, M.A. Fernández, M.R. Oliva, J.L. Soto, S. Serrano, et al., A new beta 2 microglobulin mutation found in a melanoma tumor cell line, Tissue Antigens 53 (6) (1999) 569–572.

[33] B. Seliger, D. Atkins, M. Bock, U. Ritz, S. Ferrone, C. Huber, et al., Characterization of human lymphocyte antigen class I antigen-processing machinery defects in renal cell carcinoma lesions with special emphasis on transporter-associated with antigen-processing down-regulation, Clin. Cancer Res. 9 (5) (2003) 1721–1727.

[34] Y. Nie, J. Liao, X. Zhao, Y. Song, G.Y. Yang, L.D. Wang, et al., Detection of multiple gene hypermethylation in the development of esophageal squamous cell carcinoma, Carcinogenesis 23 (10) (2002) 1713–1720.

[35] F. Locatelli, D. Pende, R. Maccario, M.C. Mingari, A. Moretta, L. Moretta, Haploidentical hemopoietic stem cell transplantation for the treatment of high-risk leukemias: how NK cells make the difference, Clin. Immunol. 133 (2) (2009) 171–178.

Generation of CD19-chimeric antigen receptor modified CD8+ T cells derived from virus-specific central memory T cells

*Seitaro Terakura,[1] *Tori N. Yamamoto,[1] Rebecca A. Gardner,[1] Cameron J. Turtle,[1,2] Michael C. Jensen,[1,3,4] and Stanley R. Riddell[1,2,5]

[1]Program in Immunology, Fred Hutchinson Cancer Research Center, Seattle, WA; [2]Department of Medicine, University of Washington, Seattle, WA; [3]Center for Childhood Cancer Research, Seattle Children's Research Institute, Seattle, WA; [4]Department of Pediatrics, University of Washington, Seattle, WA; and [5]Institute of Advanced Study, Technical University of Munich, Munich, Germany

The adoptive transfer of donor T cells that have been genetically modified to recognize leukemia could prevent or treat leukemia relapse after allogeneic HSCT (allo-HSCT). However, adoptive therapy after allo-HSCT should be performed with T cells that have a defined endogenous TCR specificity to avoid GVHD. Ideally, T cells selected for genetic modification would also have the capacity to persist in vivo to ensure leukemia eradication. Here, we provide a strategy for deriving virus-specific T cells from CD45RA−CD62L+CD8+ central memory T (T_{CM}) cells purified from donor blood with clinical grade reagents, and redirect their specificity to the B-cell lineage marker CD19 through lentiviral transfer of a gene encoding a CD19-chimeric Ag receptor (CAR). Virus-specific T_{CM} were selectively transduced by exposure to the CD19 CAR lentivirus after peptide stimulation, and bi-specific cells were subsequently enriched to high purity using MHC streptamers. Activation of bi-specific T cells through the CAR or the virus-specific TCR elicited phosphorylation of downstream signaling molecules with similar kinetics, and induced comparable cytokine secretion, proliferation, and lytic activity. These studies identify a strategy for tumor-specific therapy with CAR-modified T cells after allo-HSCT, and for comparative studies of CAR and TCR signaling. (*Blood.* 2012; 119(1):72-82)

Introduction

Allogeneic HSCT (allo-HSCT) is the most effective postconsolidation therapy for high-risk B-cell acute lymphocytic leukemia (B-ALL) in adults and can cure a fraction of pediatric and adult patients with ALL who relapse after conventional chemotherapy.[1-4] However, leukemia relapse remains a common cause of failure after allo-HSCT, and treatment of ALL that has recurred after transplant, either with additional chemotherapy or with donor lymphocyte infusions to enhance a GVL effect is mostly unsuccessful and can cause GVHD.[1-7] Thus, after transplantation therapies that augment the GVL effect without GVHD are needed to improve the survival of B-ALL patients, and could benefit other patients with aggressive B-cell malignancies that undergo allo-HSCT.[8] Adoptive T-cell immunotherapy is an attractive approach to augment the GVL effect to reduce relapse, but in the context of allo-HSCT this requires that the infused T cells specifically target leukemia cells, lack alloreactivity to avoid GVHD, and have the capacity to persist in vivo sufficiently long to eradicate all malignant cells.[9-11]

Chimeric Ag receptors (CARs) typically consist of a single-chain variable fragment (scFv) derived from a mAb specific for a tumor cell-surface molecule linked to one or more T-cell signaling moieties to activate effector function.[12,13] CAR-modified T cells can be rapidly generated by gene transfer and are MHC independent, which circumvents the need to isolate HLA-restricted tumor-specific T cells. Most B-cell malignancies including B-ALL typically express cell-surface CD19 and several groups have developed CD19-specific CARs that are

being tested in clinical trials in patients with advanced B-cell malignancies, with anecdotal reports of therapeutic activity.[14-16] The use of CAR-modified T cells could also provide a GVL effect after allo-HSCT, but it would be desirable to engineer donor T cells that have a predefined TCR specificity to avoid GVHD. The approach we have taken is to modify (CMV- and EBV-specific CD8+ T cells because large numbers of donor virus-specific T cells have previously been administered to allo-HSCT recipients without causing GVHD.[17-19] A second issue in adoptive immunotherapy is that effector T (T_E) cells that have been expanded in vitro often persist poorly in vivo, and fail to exhibit a sustained antitumor effect.[11,15,20] Our laboratory has previously identified a role for cell intrinsic properties of distinct memory T-cell subsets in determining cell fate after adoptive transfer and shown that T_E cells derived from central memory T (T_{CM}) cells not from effector memory T (T_{EM}) cells are capable of persisting long-term.[21-23] Here, we describe the development of clinical selection methods for purifying T_{CM} from peripheral blood and deriving and genetically modifying CMV- and EBV-specific T_E to express a CD19-specific CARs from the T_{CM} subset. Functional analysis of signaling through the CD19-CARs and the endogenous TCR on T_{CM}-derived bi-specific T_E cells demonstrated nearly equivalent activation of intracellular signaling pathways and activation of effector functions, including T-cell proliferation. These findings provide a strategy for performing adoptive T-cell therapy after allo-HSCT to augment the GVL effect with T cells of defined specificity and subset derivation.

- 49 -

Methods

Cell lines

Raji and K562 cell lines were obtained from the ATCC, Jeko-1 and BALL-1 were provided by Dr Oliver Press (Fred Hutchinson Cancer Research Center). TM-LCL is a CD19+ EBV-transformed lymphoblastoid cell line (LCL) that has been optimized for use as a feeder cell for T-cell culture. Cell lines were cultured in RPMI-1640 medium containing 10% FBS, 0.8mM L-glutamine, and 1% penicillin-streptomycin.

K562 cells were transduced with retroviruses that encode CD80 and CD86, and selected to > 90% purity by cell sorting for expression of these costimulatory ligands. CD80 and CD86+ K562 cells were then transduced with retroviruses that encode either a truncated cell-surface CD19 molecule or full-length HLA-A*0201 or B*0702 (Phoenix-Ampho system; Orbigen), and sorted twice to obtain cells of > 95% purity that expressed CD19 or HLA class I, respectively (supplemental Figure 1, available on the *Blood* Web site; see the Supplemental Materials link at the top of the online article). The truncated CD19 construct consisted of the entire extracellular and transmembrane domains and only 4 aa of the cytoplasmic tail to abrogate signaling after ligation.[21] Cell sorting was performed on a FACSAria (BD Biosciences). For preparation of peptide-pulsed K562/ HLA, the cells were washed once, resuspended in AIM-V medium (Invitrogen), and pulsed with the corresponding synthetic peptide at 5 μg/mL at room temperature for 2 hours. The cells were then washed once, irradiated (80 Gy), and used in stimulation assays.

Peptides

The following peptides were synthesized (GenScript) and provided at > 90% purity: VTEHDTLLY (HLA-A*0101$_{CMVpp50}$), NLVPMVATV (HLA-A*0201$_{CMVpp65}$), TPRVTGGGAML (HLA-B*0702$_{CMVpp65}$), GLCTLVAML (HLA-A*0201$_{EBV-BMLF1}$), and RAKFKQLL (HLA-B*0801$_{EBV-BZLF1}$). The peptides were dissolved in DMSO and stored at −20°C.

Separation of CD45RA⁻CD8⁺CD62L⁺ central memory T cells

Blood samples were obtained from healthy donors under protocols approved by the Fred Hutchinson Cancer Research Center Institutional Review Board. PBMCs were isolated by centrifugation of whole blood using Histopaque-1077 (Sigma-Aldrich). A CD45RA⁻CD8⁺ cell fraction was enriched by depletion of CD4⁺, CD14⁺ and CD45RA⁺ cells on the AutoMACS or CliniMACS device using clinical grade mAbs conjugated to paramagnetic beads (Miltenyi Biotec). The CD62L⁺ cells were then enriched from the depleted fraction by positive selection with a clinical grade biotin-conjugated anti-CD62L mAb (DREG56 clone; City of Hope Cancer Research Center) and anti-biotin microbeads (Miltenyi Biotec).

Lentivirus vector construction

The composition of the CD19CAR-CD28 transgene was described previously.[14] The construct was modified to contain a transduction and selection marker downstream of a T2A sequence that consisted of a truncated version of the epidermal growth factor receptor (tEGFR) that lacks the EGF binding and intracellular signaling domains.[24,25] Cell-surface tEGFR can be detected by biotinylated anti-EGFR (Erbitux) mAb.

Generation, expansion, and selection of CD19-CAR–transduced virus-specific CTLs

The enriched CD8⁺CD62L⁺ T cells were plated either in 96-well round-bottom plates at 10^4 cells/well with 10^4 autologous γ-irradiated (35 Gy), peptide-pulsed PBMCs, or at 10^6 cells/well with 10^6 autologous γ-irradiated (35 Gy) peptide-pulsed PBMCs in 24-well plates in RPMI 1640 with 10% human serum (culture medium [CM]) and 50 IU/mL IL-2. In some experiments, monocyte-derived dendritic cells

(DCs) prepared as described[26] were pulsed with peptide and used as an APC. Peptide-pulsed PBMCs and DCs were prepared by suspending the cells in AIM-V medium with the respective synthetic peptide at 5 μg/mL for 2 hours at 37°C. On day 1 after stimulation, the T cells were exposed to lentivirus supernatant encoding the CD19-CAR at a multiplicity of infection of 3 in the presence of polybrene at 2 μg/mL (Chemicon International) followed by spinfection (32°C, 500*g*, 45 minutes). On day 2, the CM was changed, and after 8-10 days of culture the cells were pooled and analyzed by flow cytometry after staining with virus-specific HLA tetramers, and with anti-EGFR and anti-Fc Abs.

The transduced T cells were expanded in culture by plating with γ-irradiated TM-LCL at various responder to stimulator ratios in CM, and fed with IL-2 50 IU/mL on days 1, 4, and 7. After 10-14 days of culture, cells were counted and stained with virus-specific HLA tetramers and Abs specific for transduction markers. The virus-specific subset of transduced T cells was then purified using reversible class I MHC streptamers as described.[27] D-biotin was added to dissociate the class I MHC streptamer from the T cells after selection.

Flow cytometry

All samples were analyzed by flow cytometry on Canto II or Calibur (BD Biosciences) instruments and the data were analyzed using FlowJo software (TreeStar). The starting PBMCs and each of the separated fractions were analyzed for CD4, CD14, CD8, CD45RA, and CD62L to determine selection purity and yield, and the final product was analyzed for CD13, CD16, CD19, and CD56 to identify the phenotype of contaminating cells. Cells were further classified by staining with CD62L, CD45RA, CD27, CD28, and CD127 mAbs (BD Biosciences) before and after culture. PE-conjugated HLA class I tetramers folded with CMV or EBV peptides were used to stain virus-specific TCRs (Beckman Coulter). Biotinylated Erbitux and streptavidin-PE were used to identify T cells that expressed tEGFR, and surface expression of the CD19-CAR was confirmed by staining with a FITC-conjugated goat anti–human Fcγ (Jackson ImmunoResearch Laboratories).

Intracellular cytokine staining

Bi-specific T_E cells were activated with either untransduced, CD19-transduced, or class I HLA-transduced and peptide-pulsed K562 cells in the presence of brefeldin A (Sigma-Aldrich), and then fixed and permeabilized with the Fix and Perm kit (BD Biosciences). After fixation, the T cells were stained with anti-IFN-γ, TNF-α, and IL-2 mAbs (BD Biosciences). Before fixation, anti-CD8 or tetramer staining was used to analyze surface coexpression of CD8 or virus-specific TCR, respectively. As a positive control for cytokine production, cells were stimulated with 10 ng/mL phorbol myristate acetate (PMA) and 500 ng/mL ionomycin (Sigma-Aldrich).

Intracellular phospho-flow analysis

Bi-specific T_E cells and K562 cells that expressed CD19 or viral peptide/ HLA complexes were mixed at a 1:5 ratio, spun down briefly, and incubated for various times at 37°C. Cells were then fixed by the addition of 2% paraformaldehyde at 37°C for 10 minutes, permeabilized in ice-cold 90% methanol, and left on ice for 30 minutes. For staining, the following phospho-specific Abs were used: CD3ζ (pY142), ZAP70 (pY292), ZAP70 (pY319)/Syk (pY352), and p38 MAPK (pT180/pY182; all PE-conjugated; BD Biosciences); Erk1/2 (pT202/pY204; ERK), and SAPK/JNK (pT183/ pY185; JNK; unconjugated; Cell Signaling Technology); bovine anti–rabbit IgG-FITC (secondary Ab; Santa Cruz Biotechnology).

Cytotoxicity assay and cytokine multiplexed bead assay

Target cells were labeled for 2 hours with ^{51}Cr, washed twice, dispensed at 2×10^3 cells/well into triplicate cultures in 96-well, round-bottom plates, and incubated for 4 hours at 37°C with CM at various E:T ratios. Percent-specific lysis was calculated using the standard formula.[28]
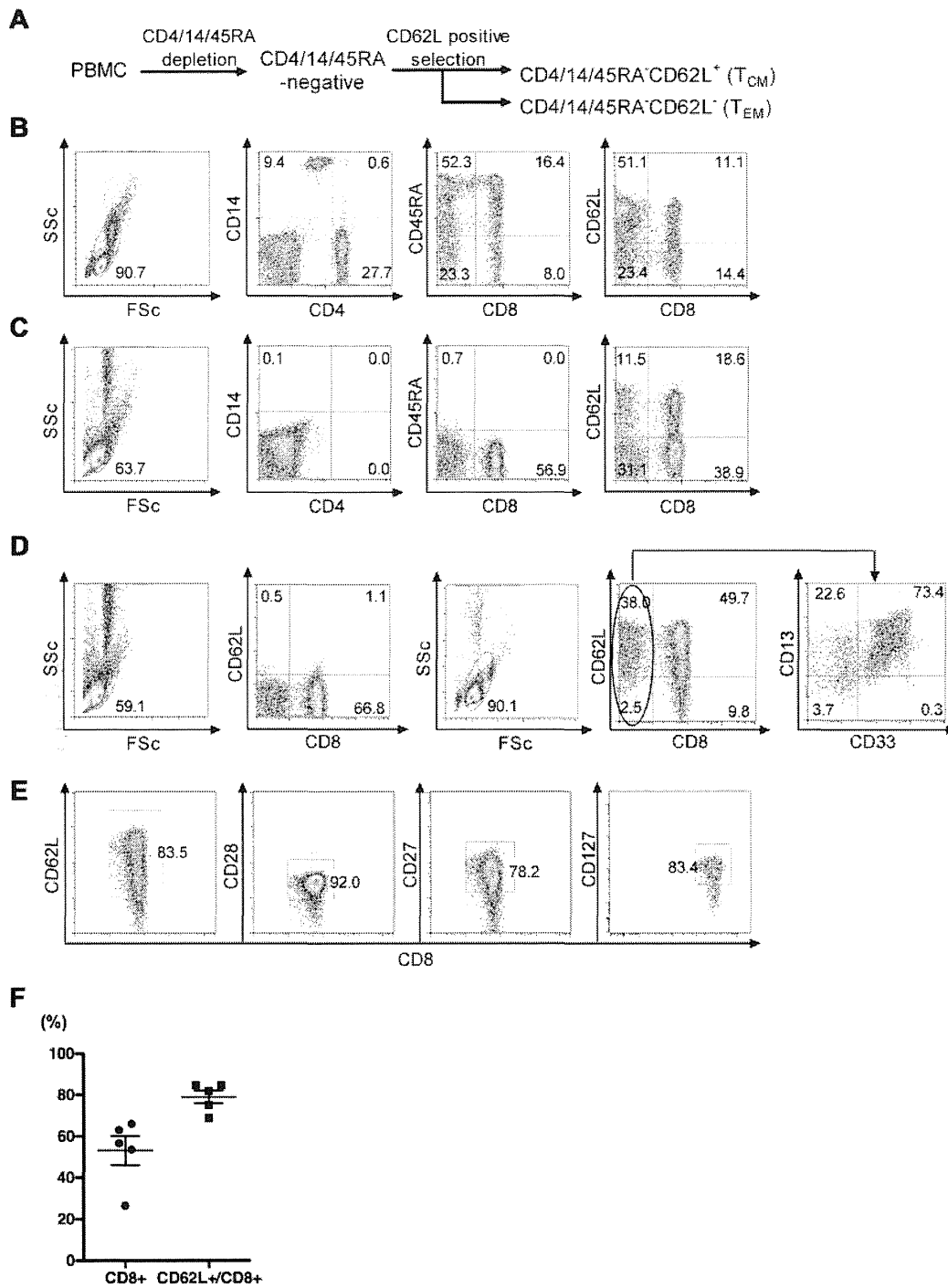
Figure 1. Enrichment of CD8$^+$ T$_{CM}$ from PBMCs with clinical grade reagents. (A) Schematic of 2-step immunomagnetic bead enrichment of CD8$^+$ T$_{CM}$. CD4$^+$/14$^+$/45RA$^+$ cells were removed from PBMCs by negative selection with directly conjugated immunomagnetic beads and CD62L$^+$ cells were then positively selected from the remaining population with a biotinylated anti-CD62L mAb and anti-biotin beads. (B) Representative flow plots of PBMC before selection showing the frequencies of CD4$^+$, CD14$^+$, CD45RA$^+$, CD8$^+$, and CD62L$^+$ cells. FSc indicates forward scatter; and SSc, side scatter. (C) Representative flow plots of the intermediate CD4/14/45RA$^-$ fraction showing removal (> 98%) of the depleted subsets. (D) Representative flow plots of the CD62L$^-$ and CD62L$^+$ fractions after the CD62L selection step. The left 2 panels show the phenotype of the CD62L$^-$ fraction and the right 3 panels show the phenotype of the CD62L$^+$ fraction. Analysis of the CD8$^-$CD62L$^+$ cells (far right panel) revealed that the most of these cells were CD13$^+$ consistent with the selection of a CD62L$^+$ myeloid subset that was not removed with the CD4/CD14/CD45RA depletion. (E) Phenotype of the CD8$^+$CD62L$^+$ fraction for markers of T$_{CM}$. Data are representative of 5 independent experiments. (F) Summary of enrichment data from independent experiments using PBMCs from 5 different donors showing the total frequency of CD8$^+$ T cells and the frequency of CD8$^+$ cells that are CD62L$^+$. The horizontal line indicates the mean ± SEM.

For analyses of cytokine secretion, target and effector cells were plated at an E:T ratio of 1:1, and IFN-γ, TNF-α, and IL-2 were measured by Luminex assay (Invitrogen) in the supernatant after 24 hours of incubation.

CFSE proliferation assay

T cells were labeled with 0.2μM CFSE (Invitrogen), washed, and plated with stimulator cells at a ratio of 1:1 in CM without IL-2. After 72- or

- 51 -

Table 1. The absolute number of target cells obtained after each selection and the yield of the target fraction

	PBMCs	CD4/CD14/CD45RA-depleted fraction	CD4/CD14/CD45RA-depleted CD62L+ fraction
Cell number	697 × 10⁶ (558-1282 × 10⁶)	31.2 × 10⁶ (23.4-38.6 × 10⁶)	8.8 × 10⁶ (7.2-13.8 × 10⁶)
% CD45RA⁻CD8⁺CD62L⁺	1.7 (0.4-3.3)	16.3 (9.2-25.7)	42.1 (22.5-55.9)*
Yield of CD45RA⁻CD8⁺CD62L⁺ cells†		45.5% (21.3%-88.4%)	25.2% (15.8%-55.5%)

*The majority of non-CD8⁺ cells were CD13⁺CD62L⁺ myeloid cells.

†The yield of CD45RA⁻CD8⁺CD62L⁺ cells was calculated by multiplying the absolute cell number of each fraction and the proportion that were CD45RA⁻CD8⁺CD62L⁺, and dividing by the absolute number of CD45RA⁻CD8⁺CD62L⁺ cells in PBMCs × 100 (%). The data are the summary of 5 experiments.

96-hour incubation, cells were labeled with anti-CD8 mAb and samples were analyzed by flow cytometry, and division of live CD8⁺ T cells was assessed by CFSE dye dilution.

Results

Enrichment of CD45RO⁺CD8⁺CD62L⁺ T_{CM} from PBMCs with clinical grade reagents

We evaluated a 2-step immunomagnetic selection method using clinical-grade reagents to enrich CD8⁺ T_{CM} from PBMCs obtained from healthy donors. CD8⁺ T_{CM} typically comprise less than 3% of PBMCs in healthy donors, and can be identified by expression of the CD45RO isoform that is acquired during the naive to memory transition, and by the coexpression of CD62L.[22,29] To enrich the CD8⁺ T_{CM} fraction, we first depleted CD4⁺, CD14⁺, and CD45RA⁺ cells from PBMCs using clinical grade mAb conjugated to paramagnetic beads, and then positively selected CD62L⁺ cells with a biotinylated anti-CD62L mAb and clinical-grade anti-biotin beads (Figure 1A). In 5 independent experiments starting with a median of 697 × 10⁶ PBMCs from different donors (Figure 1B), we obtained a median of 31.2 × 10⁶ cells (range, 23.4-38.6 × 10⁶) after the CD4/14/45RA depletion. The cells remaining after depletion contained only very rare contaminating CD4⁺/14⁺/ 45RA⁺ cells (Figure 1C), and were predominantly (> 60%) CD8⁺ T cells with a median of 16.3% CD45RA⁻ CD8⁺CD62L⁺ T_{CM} (range, 9.2%-25.7%; Table 1). After selection of CD62L⁺ cells from the CD4/14/45RA⁻ fraction, we obtained a median of 8.8 × 10⁶ (range, 7.2-13.8 × 10⁶) cells of which a median of 87.7% (range, 84.4%-93.1%) were CD62L⁺ and 56.0% (range, 29.0%-66.0%) were CD8⁺ cells. The CD8⁻ cells that remained in the CD4/14/45RA⁻CD62L⁺ fraction were primarily CD62L⁺ myeloid cells that expressed CD13 and were not removed by the initial density gradient separation (Figure 1D). The fraction of CD8⁺ T cells that expressed CD62L was 83.0% (range, 69.0%-96.0%), and these cells were predominantly CD28⁺ and CD27⁺, which is characteristic of T_{CM} (Figure 1D-F). Contaminating CD4, CD14, CD45RA, CD16, and CD19 cells were very rare in the CD4/14/45RA⁻CD62L⁺ fraction (Table 2). Thus, this 2-step immunomagnetic selection method using clinical-grade mAb-conjugated beads provided approximately 25-fold enrichment of CD8⁺ T_{CM} with an overall yield of 25.2% (range, 15.8%-55.5%; Table 1).

Enrichment of virus-specific T_E cells from T_{CM}

We next examined culture formats that would induce preferential expansion of virus-specific T cells present in the enriched T_{CM} fraction. The T_{CM} cells were cultured with CMV or EBV peptide-pulsed, γ-irradiated PBMCs in either 24-well (10⁶ responder T cells/well) or 96-well plates (10⁴ responder T cells/well), and the frequency of tetramer-positive cells was determined on day 10. The frequency of tetramer positive T cells in the starting T_{CM} population was typically low (< 0.1%) and as expected, the majority of the tetramer-positive cells were CD62L⁺ (Figure 2A, supplemental Figure 2).

Stimulation with CMV peptides presented by HLA-A*0201 and HLA-B*0702 resulted in a dramatic increase in the tetramer-positive T cells after 10 days both in the 96-well and 24-well culture formats (Figure 2A-B). Of note, the contaminating non-CD8⁺ cells that were present in the starting population declined after 10 days of culture, suggesting these cells do not persist or proliferate under these in vitro culture conditions (Figure 2A,D).

We then evaluated whether γ-irradiated, monocyte-derived DCs might be superior APCs compared with peptide-pulsed PBMCs for inducing expansion of virus-specific T_{CM} in the cultures. There was no significant difference in the frequency of tetramer-positive T cells after 10 days in cultures stimulated with peptide-pulsed PBMCs or DCs (Figure 2C). Thus, for simplicity we used PBMCs as APCs for subsequent experiments to determine whether this method would be generally effective for rapidly enriching T cells specific for multiple epitopes of EBV and CMV presented by other common HLA alleles. In all cases, we observed significant outgrowth of tetramer-positive CD8⁺ T cells, with the 24-well cultures for each of the epitopes containing > 35% tetramer-positive cells after 10 days of expansion (Figure 2D).

Lentiviral transduction of virus-specific T_{CM} and expansion of bi-specific T_E cells

The selective outgrowth of virus-specific T_{CM} after Ag stimulation suggested it might be possible to simultaneously transduce the cells with a CD19-CAR lentivirus during their proliferation to rapidly derive bi-specific T cells. Therefore, we stimulated CD8⁺ T_{CM} with peptide-pulsed PBMCs and added lentivirus supernatant on day 1 followed by spinfection (Figure 3A). After 8-10 days, the cells were examined for tetramer staining to determine the frequency of virus-specific T cells, and for expression of the CAR and tEGFR to determine the frequency of transduced T cells. In 6 independent experiments, the fraction of cells that were tetramer positive was a median of 30.1% (range, 5.8%-94.7%), and the fraction that expressed the CD19-CAR was a median of 21.5% (range, 11.7%-27.9%). A median of 54.9% (range, 15.7%-96.1%) of the tetramer-positive T cells was also CD19-CAR⁺ as assessed by staining for either the Fc portion of the CAR or tEGFR, which is encoded downstream of a T2A sequence in the CAR vector and coordinately expressed with the CAR (Figure 3B). The majority of cultures had only a very minor population of Fc or tEGFR⁺, tetramer-negative cells (Figure 3B). The selective transduction and expansion of virus-specific T cells was observed after stimulations with multiple CMV epitopes (HLA-A*0101$_{CMVpp50}$; HLA-A*0201$_{CMVpp65}$; HLA-B*0702$_{CMVpp65}$) and with EBV epitopes (HLA-A*0201$_{EBV-BMLF1}$; HLA-B*0801$_{EBV-BZLF1}$). Thus, simultaneous Ag stimulation and lentiviral transduction was successful in reproducibly deriving a population of T cells that expressed both a virus-specific TCR and a CD19-CAR.

We next evaluated whether subsequent stimulation of the cultures with CD19⁺ APCs would expand the CD19-CAR⁺ T cells and retain the dominant virus-specific fraction. We evaluated an
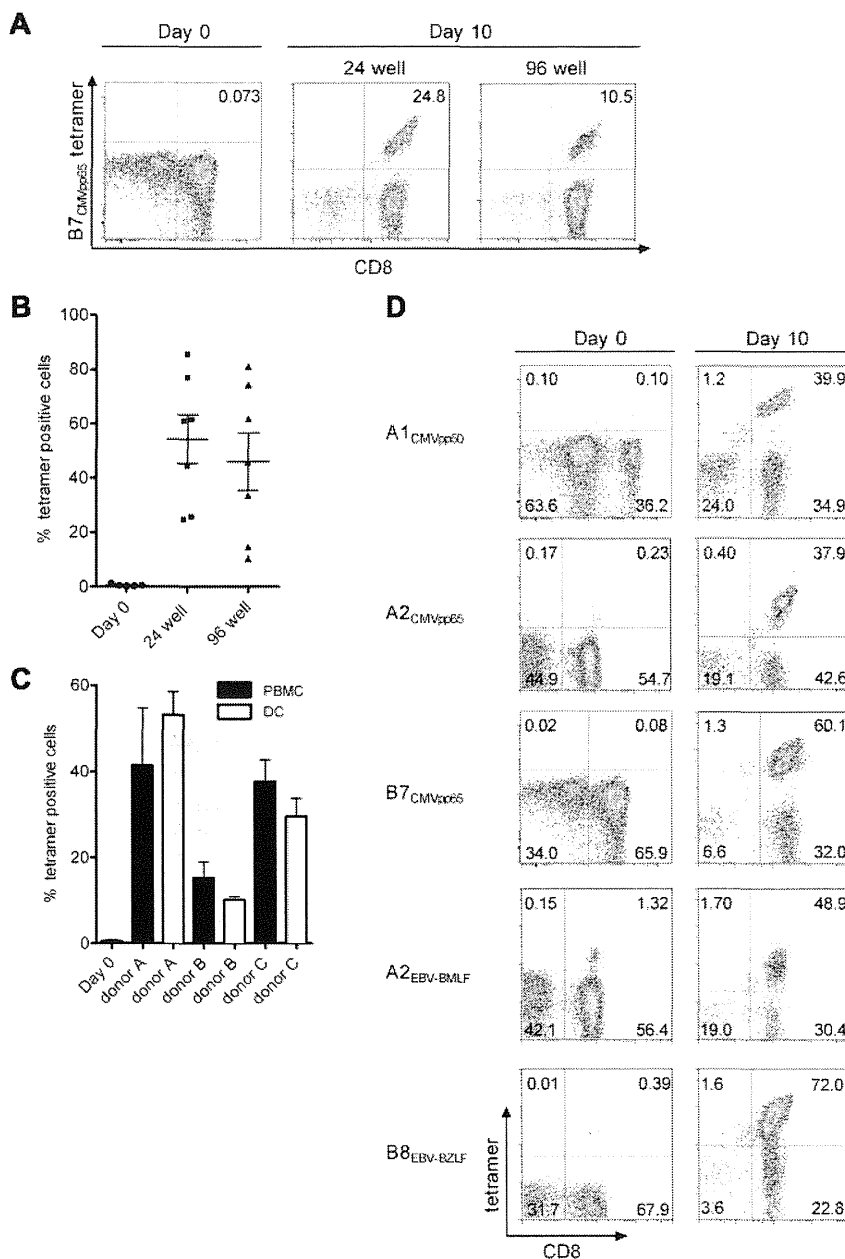
Figure 2. Comparison of culture conditions for expanding virus-specific T cells from CD45RA⁻CD62L⁺CD8⁺ precursors. (A) Representative flow plots showing tetramer staining of the enriched CD8⁺CD62L⁺ T_{CM} before and 10 days after stimulation with a B*0702$_{CMVpp65}$ peptide. T_{CM} cells were plated either in a 24-well or 96-well plate with B*0702$_{CMVpp65}$ peptide-pulsed γ-irradiated PBMCs. Shown are data from individual wells of the 24-well cultures and pooled wells of the 96-well cultures. (B) T_{CM} cells from 7 donors were cultured the same as in panel A and tested for tetramer positivity on day 10. T_{CM} from 3 donors were stimulated with an A*0201$_{CMVpp65}$ peptide, and T_{CM} from the other 4 donors were stimulated with a B*0702$_{CMVpp65}$ peptide. Symbols represent the frequency of tetramer-positive T cells in cultures from each individual donor and the horizontal lines indicate the mean ± SEM. (C) T_{CM} cells were plated onto 96-well plates and stimulated with either peptide-pulsed PBMC (■) or peptide-pulsed DCs (□). After 10 days of culture, 6 to 12 wells with growth were randomly selected and analyzed for the frequency of virus-specific T cells by tetramer staining. For each of the 3 donors, a B*0702$_{CMVpp65}$ peptide was used for stimulation. The graph shows the mean frequency of tetramer positive cells in each donor and SEM at day 10 after each stimulation condition. (D) T_{CM} cells from 4 donors were plated with autologous PBMCs pulsed with CMV or EBV peptides known to be presented by HLA alleles of the donor. The frequency of virus-specific T cells was determined by tetramer staining in the starting population and 10 days after stimulation. Data are representative of 5 independent experiments from each donor.

EBV-transformed LCL line (TM-LCL) that is CD19⁺, HLA-A2 and -B7 negative, and used widely to provide feeder cells for expanding human T cells for clinical adoptive therapy.[30,31] We tested a range of responder-stimulator ratios and found that a T cell:LCL ratio of 1:7 gave the greatest expansion of CD19-CAR⁺ T cells (Figure 3C), with a total cell yield of > 10^{10} T cells more than 2 cycles of stimulation starting from 10^6 cells. The percentage of tetramer-positive T cells in the cultures increased similar to CAR-transduced cells despite the absence of stimulation through the virus-specific TCR, although there was variability from culture to culture (Figure 3D right panel).

Purification of bi-specific T_E cells using class I MHC streptamers

T cells specific for CMV and EBV, either selected by in vitro culture or with class I MHC streptamers, have been adoptively transferred to allo-HSCT recipients without causing GVHD.[17,18,32] Thus, if donor-derived CD19 CAR-modified T cells were to be administered for adoptive immunotherapy to prevent or treat relapse of CD19⁺ malignancies in the allo-HSCT setting, it would be desirable to infuse T-cell products that were predominantly virus specific. Thus, we used reversible class I MHC streptamers to further purify virus-specific T cells from the

Table 2. Contaminating cell frequencies in CD45RA⁻CD8⁺CD62L⁺ fraction

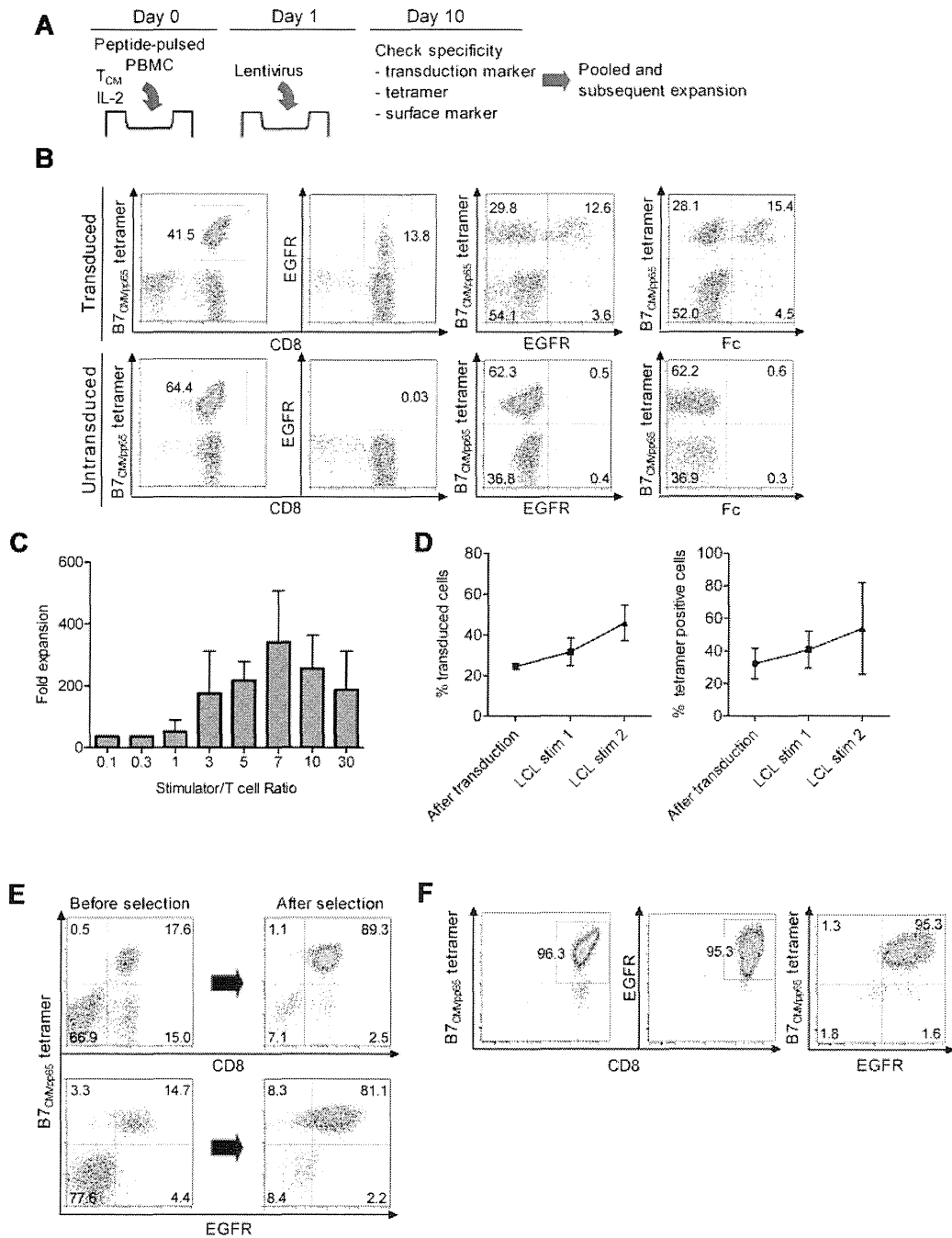|	Median, %	Range, %
CD4	0.6	0.1-2.9
CD14	0.1	0.1-2.0
CD45RA	1.0	0.0-3.2
CD13	31.4	23.2-69.5
CD16	2.0	0.1-6.8
CD19	0.1	0.1-0.3

Figure 3. Lentiviral transduction, expansion, and selection of bi-specific T cells. (A) Scheme for simultaneous virus-specific stimulation and CD19-CAR transduction. T_{CM} cells were plated at 10^6 cells/well into 24-well plates with 10^6 peptide-pulsed γ-irradiated PBMCs/well and IL-2 (50 IU/mL), and transduced on day 1 with CD19-CAR lentivirus supernatant. (B) Staining of transduced and untransduced T cells with HLA tetramer, anti-Fc, and anti-EGFR reagents after 10 days of culture. Data are shown for a culture stimulated with an HLA-B*0702$_{CMVpp65}$ peptide-pulsed PBMCs. Similar data were obtained for T_{CM} cells stimulated with A*0101$_{CMVpp50}$, A*0201$_{CMVpp65}$, A*0201$_{EBV-BMLF1}$, and B*0801$_{EBV-BZLF1}$ peptides. (C) Growth of bi-specific T cells after stimulation with CD19⁺ EBV-transformed B cells (TM-LCL) at various T-cell:LCL ratios during a 10-day stimulation cycle. Data are pooled from 5 independent experiments and the mean fold expansion in cell number and SEM are shown. (D) CD19-CAR⁺ and tetramer-positive T cells are enriched over 2 cycles of stimulation with CD19⁺ TM-LCL. The bi-specific T cells were stimulated with a 1:7 ratio of TM-LCL, fed with 50 IU/mL IL-2 and the frequency of cells that bound the HLA tetramer and expressed cell-surface EGFR was determined on day 10-13 (left panel, CAR⁺ cells; right panel, tetramer-positive cells). Data are pooled from 5 independent experiments (mean and SEM) with 4 viral epitopes (A*0101$_{CMVpp50}$, A*0201$_{CMVpp65}$, B*0702$_{CMVpp65}$, and A*0201$_{EBV-BMLF1}$). (E) Purification of tetramer positive bi-specific cells with reversible class I MHC streptamer. Streptamer selection was performed after the first stimulation with CD19⁺ TM-LCLs. Shown are the data for selection of HLA B*0702$_{CMVpp65}$ bi-specific T cells, which is representative of 4 independent experiments with A*0101$_{CMVpp50}$, A*0201$_{CMVpp65}$, B*0702$_{CMVpp65}$, and A*0201$_{EBV-BMLF1}$ streptamers. The yield was a median of 26.9% (range, 15.0%-43.8%). (F) Purity of final bi-specific T_{CM}-derived cell product. After MHC streptamer selection, a second stimulation with TM-LCL was performed and the bi-specific T cells were stained with the class I HLA tetramer and with anti-EGFR on day 10 after stimulation. Data are shown for a bi-specific (B*0702$_{CMVpp65}$; CD19CAR) T-cell product and are representative of 4 independent experiments.

transduced T-cell cultures after the first stimulation with CD19⁺ LCL.[27] Streptamer selection resulted in the reproducible enrichment of virus-specific T cells to > 80% purity (range, 86.0%-96.8%), of which ~ 85% (range, 80.0%-99.7%) expressed the CD19-CAR. The overall cell yield with streptamer selection was a median of 26.9% (range, 15.0%-43.8%). Importantly, the
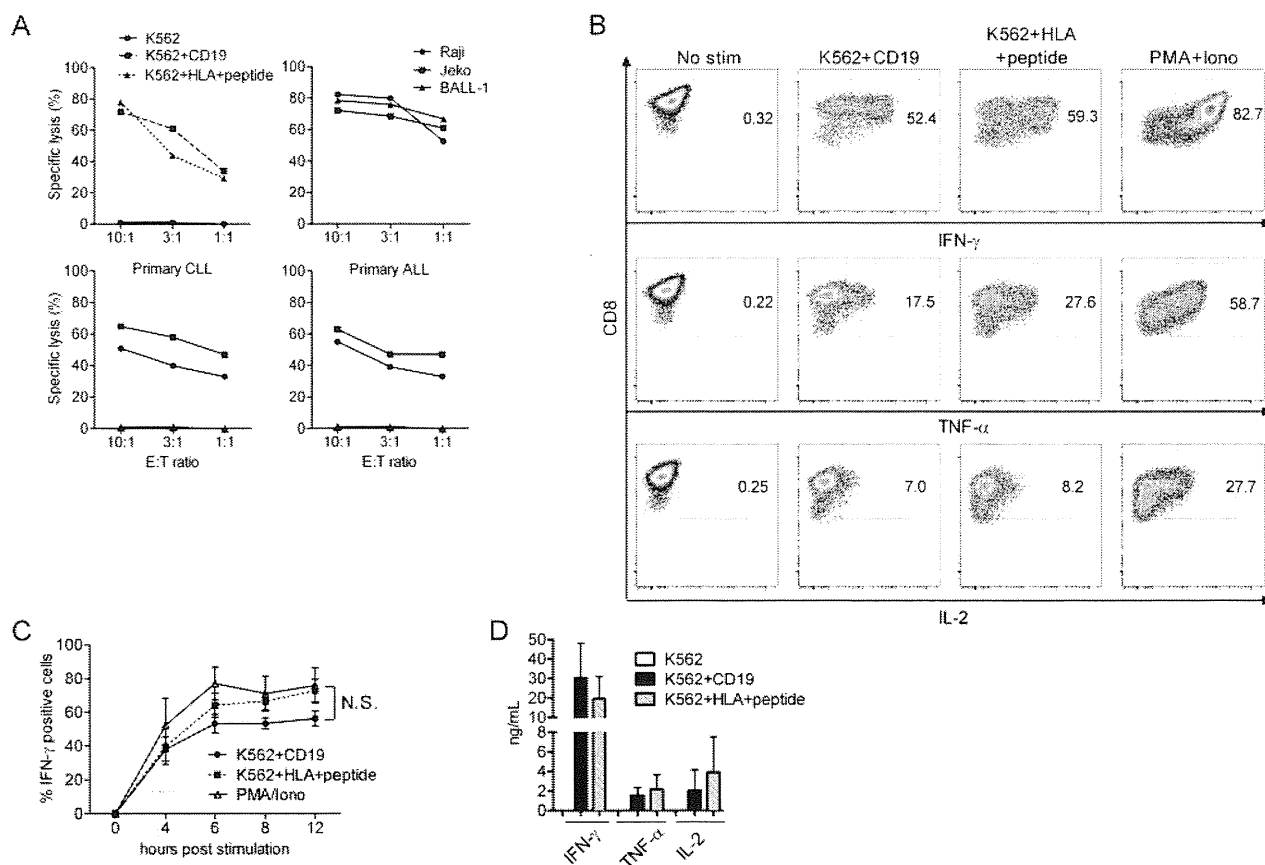
Figure 4. Analysis of effector functions after stimulation of bi-specific T cells through the virus-specific TCRs and CD19-CARs. (A) Cytotoxicity. HLA-B*0702$_{CMVpp65}$ bi-specific T cells were tested for lysis of K562 (●), K562 transduced with CD19 (■), and K562 transduced with HLA-B*0702 and pulsed with CMVpp65 peptide (▲; top left panel). Bi-specific T cells lysed CD19+ tumor cell lines (top right panel), primary CLL cells from 2 patients (bottom left panel) and primary ALL cells from 2 patients (bottom right panel). In assays against primary tumor cells, K562 cells were used as a negative control (triangles in the bottom panels). (B) Intracellular cytokine staining. HLA-B*0702$_{CMVpp65}$ bi-specific T cells stimulated for 4 hours with an equal number of the indicated K562 transfectants, permeabilized, and stained for intracellular IFN-γ, TNF-α, and IL-2, or left unstimulated. Stimulation with PMA/ionomycin served as a positive control. Data are shown for B*0702$_{CMVpp65}$ bi-specific T cells and are representative of 5 experiments with bi-specific T cells from different donors. (C) Time-course analyses of intracellular IFN-γ staining of the bi-specific T cells. T cells were stimulated either with the indicated K562 transfectants or with PMA/ionomycin for 4-12 hours, permeabilized, and stained for intracellular IFN-γ. The mean and SEM of the percentage of T cells that stained positive for IFN-γ is shown for 5 independent experiments with bi-specific T cells from 3 donors (N.S., not significant). (D) IFN-γ, TNF-α, and IL-2 secretion. T cells were stimulated with the indicated K562 transfectants at a 1:1 ratio, and culture supernatants were harvested at 24 hours and analyzed by Luminex assay. Data are pooled from 7 independent experiments with bi-specific T cells from 7 donors (mean and SD).

frequency of CD19-CAR–transduced T cells in the selected population that did not stain with the tetramer was < 3% (Figure 3E).

After the streptamer selection, a second stimulation with CD19+ LCL was performed to determine whetherthe high frequency of bi-specific T cells was maintained through an additional expansion cycle. The T cells proliferated equivalently well as those that had not undergone streptamer selection and at the end of the stimulation cycle, the frequency of tetramer-positive and CD19-CAR+ cells in the culture increased to ~ 90% (range, 80.7%-96.3%) and ~ 85% (range, 77.9%-95.3%), respectively (Figure 3F). Thus, large numbers of highly pure bi-specific T$_E$ cells that are derived from CD8+ T$_{CM}$ precursors and engineered to express a CD19-specific chimeric receptor could be readily generated for adoptive immunotherapy of allo-HSCT recipients in ~ 30-35 days starting from 400 mL of donor peripheral blood.

Analysis of effector functions, signaling, and cell division after stimulation through the virus-specific TCR and CD19-CAR

Prior studies have demonstrated that polyclonal T cells transduced to express a CAR can lyse target cells and secrete cytokines after

stimulation through the CAR, and that incorporation of costimulatory domains such as CD28, 4-1BB, and OX40 into the CAR increases IL-2 production and improves the persistence of the cells in immunodeficient mice.[14,33] However, CAR binding to its ligand is expected to be structurally distinct from that of a TCR, and a direct comparison of effector functions and signaling through an introduced CAR and the endogenous TCR on the same cell has not been evaluated. To perform this analysis, we transduced K562 tumor cells with the costimulatory molecules CD80 and CD86, and with CD19 or HLA molecules (HLA-A*0201; HLA-B*0702) and sorted cells that expressed each of the transgenes to high purity (> 95%; supplemental Figure 1). The bi-specific T cells that we generated in our cultures efficiently lysed both K562/CD19 and K562/HLA viral peptide-pulsed target cells, in addition to CD19+ tumor cell lines, primary CD19+ chronic lymphocytic leukemia (CLL) and ALL cells, indicating that lytic function was mediated through both the CAR and the TCR (Figure 4A). IFN-γ, TNF-α, and IL-2 production after ligation of the CD19-CAR or the TCR was evaluated by stimulating aliquots of the bi-specific T cells with each of the K562 transfectants. K562/B*0702$_{CMVpp65}$ stimulation induced a slightly higher percentage of bi-specific T cells to